

# Constitutional Isomers of Dendrimer-like Star Polymers: Design, Synthesis and Conformational and Structural Properties\*

**Mikael Trollsås, Bjorn Atthöf, Andreas Würsch, James L Hedrick**

IBM Almaden Research Center, 650 Harry Road, San Jose, CA 95120

**John A Pople**

Stanford Synchrotron Radiation Laboratory,

Stanford Linear Accelerator Center, Stanford University, Stanford, CA 94309

**Alice P Gast**

Dept. of Chemical Engineering, Stanford University, Stanford, CA 94305

## *Abstract*

The design, synthesis and solution properties of six constitutional isomers of dendrimer-like star polymers is described. Each of the polymers have comparable molecular weights ( $\sim 80,000$  g/mol), narrow polydispersities ( $< 1.19$ ) and an identical number of branching junctures (45) and surface hydroxyl functionalities (48). The only difference in the six isomers is the placement of the branching junctures. The polymers are constructed from high molecular weight poly( $\epsilon$ -caprolactone) with branching junctures derived from 2,2'-bis(hydroxymethyl) propionic acid (bis-MPA) emanating from a central core. The use of various generations of dendritic initiators and dendrons coupled with the ring opening polymerization of  $\epsilon$ -caprolactones allowed a modular approach to the dendrimer-like star polymer isomers. The most pronounced effects on the physical properties/morphology and hydrodynamic volume was for those polymers in which the branching was distributed throughout the sample in a dendrimer-like fashion. The versatility of this approach has provided the possibility of understanding the relationship between architecture and physical properties. Dynamic light scattering and small angle X-ray scattering techniques were used to determine the hydrodynamic radius  $R_h$  and radius of gyration  $R_g$  respectively. The relationship between  $R_g$  and molecular weight was indicative of a compact star-like structure, and did not show advanced bias towards either the dense core or dense shell models. The radial density distribution of the isomers was therefore modeled according to a many arm star polymer, and good agreement was found with experimental measures of  $R_h / R_g$ .

*Submitted to Macromolecules*

---

\* Work supported by Department of Energy contract DE-AC03-76SF00515

## INTRODUCTION

The control of polymer properties through the synthesis of complex macromolecular architectures is central to many areas of research and advanced technological applications.<sup>1</sup> Properties of organic materials are altered mainly through modification of their *constitution*.<sup>2</sup> Examples of constitutional changes include the use of different monomers, variable molecular weights, polydispersities, block and graft copolymers. Advances in living and controlled polymerization techniques has facilitated the preparation of these materials.<sup>3</sup> The variation of the macromolecular architecture is another example of a constitutional change that exerts a considerable influence on the material properties:<sup>1b</sup> for example, many of the mechanical, rheological and related material properties can be correlated to the type and degree of branching. Nearly a decade ago, a new class of macromolecules denoted as dendrimers emerged and provided a model for investigation of the solution and physical properties of materials with precisely defined branched structures.<sup>4,5</sup> The use of new multifunctional initiators coupled with the new polymerization techniques has also provided the availability of new high molecular weight materials with a wide variety of macromolecular architectures including star-shaped polymers, which have been shown to have lower hydrodynamic volumes and lower melt viscosities than their linear counterparts.<sup>6</sup>

Constitutional isomers are molecular compounds that differ in the nature of the functional group, e.g.,  $\text{CH}_3\text{CH}_2\text{OH}$  and  $\text{CH}_3\text{OCH}_3$ , or in the position of an atom or a group, e.g., 1-propanol and 2-propanol, or in the nature of the skeletal structure, e.g., n-butane and i-butane.<sup>2</sup> Since the chemical structure of constitutional isomers can be very different, the effect on the chemical, physical and biological properties can also be considerable. One example of polymeric constitutional isomers is poly(ethylene oxide) and poly(vinyl alcohol), and although these materials have comparable solution behavior (i.e., water solubility), they manifest completely different physical properties. Likewise, poly(lactides) prepared from the ring-opening polymerization of the cyclic diester monomer represent another example of constitutional isomers.<sup>7</sup> The cyclic lactide monomer (i.e., cyclic diester) contains two chiral centers which creates the possibility of two diastereomers, L- and D-lactide and a meso compound, *meso*-lactide. Polymers derived from L-lactide are semi-crystalline, whereas polymers derived from the *rac*-monomer are amorphous, and these widely different physical properties dictate their applications. The most important example is poly(ethylene), the most commonly used bulk polymer, which exists either as linear low density poly(ethylene) (LDPE), as high density polyethylene (HDPE), or, (as has been allowed by more recent synthetic advances), highly branched or amorphous poly(ethylene). All of these differ only in the nature of the skeletal structure,<sup>8</sup> yet it is well known that LDPE and HDPE have significantly different mechanical properties due to their different extent of crystallization. However, owing to the broad polydispersity of these constitutional isomers, determination of precise relationships between structure and properties on the affects of branching is difficult.

Although considerable data has been generated on materials with different branching extents, few have utilized living polymerization methods to generate materials with controlled and precisely defined architectures with narrow polydispersities. This stems primarily from the limited polymerization methods available for the preparation of well-defined, narrowly dispersed and branched macromolecules. In one elegant study addressing this problem, Hawker et al.<sup>9</sup> synthesized the exact linear analog of the different generations of benzyl ether dendrimers in a stepwise approach. In this investigation, the molecular architectures were shown to have a

significant influence on the hydrodynamic volume as well as the physical properties of the oligomers to molecular weights to 6,700 g/mol. The scaling of the hydrodynamic volume of the branched macromolecule with molecular weight showed a significant deviation from the linear analog between the fourth and fifth generations, consistent with reports on other properties for dendrimers.<sup>10</sup>

A new class of materials are dendrimer-like star polymers.<sup>11</sup> These polymers are interesting since controlled branching can be introduced in materials with molecular weights up to 250,000 g/mol. In addition, they enable variation in the degree of polymerization and degree of branching as well as the preparation of block and amphiphilic copolymers. Dendrimer-like star polymers have primarily been based on the living ring-opening polymerization (ROP) of lactones and lactides with derivatives of 2,2'-bis(hydroxymethyl) propionic acid (bis-MPA) as branching junctures and dendritic initiators. Similar dendritic structures have also been prepared from poly(ethylene oxide)<sup>6h</sup> and poly(methyl methacrylate) and related vinyl monomers via atom transfer radical polymerization (ATRP).<sup>11d</sup> The preparation of dendrimer-like star polymers based on three generations of  $\epsilon$ -caprolactone with varying degrees of polymerization (DP = 5, 10, 15, 20) for each generation, allowed the possibility of distinguishing the unique characteristics of dendrimer-like star polymers, dendrimers and star polymers.<sup>11e,f</sup> It was shown for the dendrimer-like star polymers that if the DP is 10 or higher, three generations of polymer were required to obtain a material with lower hydrodynamic volume than the traditional star polymers. Moreover, the versatility of the synthetic procedure to dendrimer-like star polymers has permitted variations in the molecular structure between the different generations (i.e., lactide, methyl methacrylate, substituted lactones, etc.), which has enabled the preparation of both amorphous and semi-crystalline materials<sup>11e,f</sup> as well as materials that undergo microphase separation. For example, the preparation of optically active materials has been demonstrated by the incorporation of either L- or D-lactide. By using optically active lactide as the monomer in one, two or all generations in the polymers, it was shown that the optical activity is identical in all layers.<sup>11g</sup> This, in turn, provided another means of verifying the composition and structure of the dendrimer-like star polymers and copolymers. In another report, block copolymers were prepared using amorphous dendrons of bis-MPA as the second layer organization.<sup>11</sup>

The characterization of the radial density profiles and radii of gyration of dendrimers and dendrimer-like polymers has received some attention in the literature to date.<sup>12</sup> Early Monte-Carlo studies of dendrimer macromolecules based on the diamond lattice model predicted that dendrimers beyond the fourth generation would exhibit some hollowness at the core, and that the radius of gyration  $R_g$  would increase approximately linearly with the generation number.<sup>12a</sup> More recent work rejected the earlier finding of hollow cored dendrimers:<sup>12c</sup> Models considering atomic level force fields by Grest suggested that the dendrimers would remain as compact (space-filled) structures, irrespective even of the solvent conditions, and that therefore  $R_g$  would scale with the cube root of the number of monomers.<sup>12b</sup> Other workers find that  $R_g$  scales according to a power law dependence of the generation number:  $R_g \propto G^{1-v}$  for generation number G and Flory exponent v.<sup>12d</sup>

Experimental characterization of the radial density profile and radius of gyration of dendrimer-like polymer systems is limited.<sup>12e-g</sup> A small angle X-ray scattering (SAXS) study of poly(propyleneimine) dendrimers in solutions of methanol by Prosa *et al.* indicated that the density profile remained relatively unaffected by the dendrimer generation, between the third and tenth generations.<sup>12e</sup> A small angle neutron scattering (SANS) study of poly(propyleneimine)

dendrimers in aqueous solution by Scherrenberg and coworkers revealed that the dendrimers behaved as soft molecules with possible interpenetration at higher concentration.<sup>12f,g</sup> Electrostatic repulsion dominated as the solvent pH was lowered resulting in a stretching of the molecules and a behavior more characteristic of harder particles.<sup>12f</sup> It was further shown that the dimension of the dendrimers increased linearly with the generation number (roughly as  $M^{1/3}$ , where M is the number average molecular weight) independent of the character of the end group and of the solvent used.<sup>12g</sup> The dendritic polymer was thus concluded to be in a folded, rather than extended, conformation, exhibiting a relatively homogeneous density distribution. We have performed initial studies on the first three generations of dendrimer-like caprolactone star polymers, which indicate that  $R_g$  scales non-linearly with generation number,<sup>11c</sup> and with an exponent smaller than that proposed in the model of Chen and Cui.<sup>12d</sup> We also found that an increase in the degree of polymerization of the star arms does not significantly increase  $R_g$ .<sup>11c</sup> In this study we report measures of  $R_g$  for six constitutionally isometric  $\epsilon$ -caprolactone based dendrimer-like star polymers and consider the radial densities of each of the isomers as a function of their differing architectures. Each of the polymers have comparable molecular weights, narrow polydispersities as well as identical number of branching junctures and surface functional groups. The synthesis of the dendrimer-like star polymers will be discussed together with the basic structure-property relationships that stem from these similar but different architectures. To our knowledge, this constitutes one of the few studies of macromolecular isomerism on a carefully designed series of high molecular weight polymers.

## EXPERIMENTAL

### Materials

Stannous-2-ethylhexanoate ( $Sn(Oct)_2$ ) (Sigma) and all other chemicals (Aldrich) were purchased and used without any further purification, except for the  $\epsilon$ -caprolactone which was dried over  $CaH_2$  for 24 h and then distilled under high vacuum before use. The hydroxyl-functional dendrimers were synthesized according to a procedure developed by Hult et al.<sup>13</sup> The synthesis of 2,2'bis(phenyldioxymethyl) propionic acid, 1, was prepared according to a literature procedure.<sup>11a</sup>

### Techniques

$^1H$ -NMR were recorded in  $CDCl_3$  solution, on a Bruker AM 250 (250 MHz) apparatus with the solvent proton signal for reference.  $^{13}C$ -NMR spectra were recorded at 62.9 MHz on the same instrument using the solvent carbon signal as a reference. All polymer  $^{13}C$ -NMR spectra were recorded on 250 mg of sample using 16384 scans. The number average molecular weights of the polymers were calculated from the  $^1H$ -NMR data.<sup>11a</sup> The molecular weight distributions were determined by size exclusion chromatography (SEC) using a Waters chromatograph connected to a Waters 410 differential refractometer and an UV-detector. Four 5 $\mu$ m Waters columns (300 · 7.7 mm) connected in series in order of increasing pore size (100, 1000,  $10^5$ ,  $10^6\text{\AA}$ ) were used with THF as solvent at 25 °C. Poly(styrene) standard samples were used for calibration.

Dynamic light scattering (DLS) measurements were performed at Stanford University with an argon ion laser at a power of 0.8W and an excitation wavelength of  $\lambda = 514.5$  nm. The scattered light intensity was measured at an angle of 90.0 degrees. Samples were prepared as 1 wt% polymer in solution with THF. Samples were sonicated for 30 minutes and transferred via a syringe into glass fluorescence cells, through a 100nm filter. The cells had been cleaned by

soaking overnight in 70/30 vol.% sulfuric acid/hydrogen peroxide solution, and rinsed first with water and then filtered THF. Data acquisition was performed using a Brookhaven Instruments BI-9000 correlator: data collection cycles lasted 10 minutes. The temperature of the solutions was maintained at 25 °C by a circulating bath.

For a system with a distribution of sizes, the autocorrelation function  $g^{(1)}(q, \tau)$  takes the form <sup>14a</sup>

$$g^{(1)}(q, \tau) = \int_0^{\infty} F(R_h) \exp\left[-\frac{q^2 kT}{6\pi\mu} R_h^{-1} \tau\right] dR_h + \Delta \quad (1)$$

The characteristic decay times of the autocorrelation function depend on parameters such as the solution viscosity  $\mu$  and the thermal energy  $kT$ . Scattering from large impurities such as dust is incorporated in the autocorrelation function as an additive “dust term”  $\Delta$ . Filtered samples were noted generally to be dust-free.

The  $R_h$  distribution is weighted by the intensity  $F(R_h)$ . The autocorrelation data was analyzed using CONTIN, <sup>14b-c</sup> a FORTRAN program performing a constrained Laplace transform of the data to find an optimum  $F(R_h)$  size distribution which, when used with Equation 1, causes  $g^{(1)}(q, \tau)$  to fit best the data. The CONTIN program also integrates over each peak in the size distribution to find a weighted average  $\bar{R}_h$  for each peak.

Small angle X-ray scattering was performed on beamline 1-4 of the Stanford Synchrotron Radiation Laboratory (SSRL) at the Stanford Linear Accelerator Center (SLAC), in Stanford, CA. The facility offers a focused, collimated X-ray source with a flux of  $10^{10}$  photons on a spot size of ~ 0.5mm (vertical) x 1mm (horizontal), monochromated by a 1 1 1 Si crystal to a wavelength of  $\lambda = 1.488\text{\AA}$ . The solutions were mounted in a holder manufactured at SSRL with 25  $\mu\text{m}$  thick ruby mica windows with an active path length of 1mm. 16 bit SAXS data were collected at room temperature on 2 dimensional image plates with 800x800 pixels. These data were corrected for background scattering and scattering from the sample cell. 1 dimensional profiles of the data were acquired by radial integration routines. The  $q$  range sampled was  $0.01 < q < 0.25 \text{\AA}^{-1}$ , (where  $q$  is the scattering vector:  $q = 4\pi \sin \theta / \lambda$ , for photons of wavelength  $\lambda$  scattered through an angle  $2\theta$ ).

## SYNTHESIS

### 2,2-Bis(tert-butyldimethylsiloxyane) benzyl propionate, g1(-CO<sub>2</sub>C<sub>7</sub>H<sub>7</sub>-TBDMS), 3.

2,2-Bis(hydroxymethyl) benzyl propionate, **2** (49.8 g, 222 mmol), tert-butyldimethylsilyl chooride (TBDMSCl) (80. δ 5 g, 535 mmol) and imidazole (37.8 g, 533 mmol) were dissolved in CH<sub>3</sub>CN (150 ml). The mixture was stirred for 12 h and the solvent was evaporated. The crude product was dissolved in hexane and extracted with H<sub>2</sub>O. The organic phase was separated and dried (MgSO<sub>4</sub>). The hexane was evaporated to yield 95.2 g (94%) of a colorless liquid. <sup>1</sup>H-NMR (CDCl<sub>3</sub>) δ 0.00 (s, 12H, -Si(CH<sub>3</sub>)<sub>2</sub>), 0.83 (s, 18H, -C(CH<sub>3</sub>)<sub>3</sub>), 1.12 (s, 3H, -CH<sub>3</sub>), 3.64–3.77 (1, 4H, -CH<sub>2</sub>O-), 5.10 (s, 2H, -CH<sub>2</sub>-), 7.32 (2, 5H, -Ph).

### 2,2-Bis(tert-butyldimethylsiloxyane) propionic acid, g1(-COOH, -TBDMS), and a general procedure for the removal of the benzyl group, 4.

g1(-CO<sub>2</sub>C<sub>7</sub>H<sub>7</sub>, -TBDMS) (210 mmol, 95.2 g) was dissolved in EtOAc (100 ml) and Pd/C (10 wt%) (1.5 g) was added. The apparatus for catalytic hydrogenolysis was filled with H<sub>2</sub>(g). The reaction mixture was shaken, and the deprotection was stopped after completion

(approximately 4h) and the Pd/C was filtered off. The solvent was evaporated to yield 94.2 g (99%) of a colorless liquid.  $^1\text{H-NMR}(\text{CDCl}_3)$   $\delta$  0.00 (s, 12H,  $-\text{Si}(\text{CH}_3)_2$ ), 0.82 (s, 18H,  $-\text{C}(\text{CH}_3)_3$ ), 1.07 (s, 3H,  $-\text{CH}_3$ ), 3.60–3.69 (q, 4H,  $-\text{CH}_2\text{O}-$ ).  $^{13}\text{C-NMR}(\text{CDCl}_3)$   $\delta$  –5.62, 17.05, 18.18, 25.77, 49.69, 64.39, 179.44.

**g2(-CO<sub>2</sub>C<sub>7</sub>H<sub>7</sub>, -TBDMS) and a general procedure for the DCC esterification, 5.**

2,2-Bis(hydroxymethyl) benzyl propionate (23.3 g, 104 mmol), **g1(-COOH, -TBDMS)** (79.0 g, 218 mmol) and 4-(dimethylamino) pyridinium (DPTS) (4.87 g, 15.5 mmol) were dissolved and stirred in CH<sub>2</sub>Cl<sub>2</sub>, dicyclohexyl carbodiimide (DCC) (55.7 g, 0.270 mmol) was then added and the mixture was left to react for 12 h. The mixture was filtered and the filtrate was purified by column chromatography (silica gel, hexane/EtOAc 95:5 as eluent). The yield was 30 g (32%) of a viscous and colorless liquid.  $^1\text{H-NMR}(\text{CDCl}_3)$   $\delta$  0.00 (s, 24H,  $-\text{Si}(\text{CH}_3)_2$ ), 0.84 (s, 36H,  $-\text{C}(\text{CH}_3)_3$ ), 1.09 (s, 6H,  $-(\text{CH}_3)_2$ ), 1.23 (s, 3H,  $-\text{CH}_3$ ), 3.56–3.70 (q, 8H,  $-\text{CH}_2\text{O}-$ ), 4.15–4.30 (1, 4H,  $-\text{CH}_2\text{O}-$ ), 5.13 (s, 2H,  $-\text{CH}_2-$ ), 7.33 (s, 5H,  $-\text{Ph}$ ).  $^{13}\text{C-NMR}(\text{CDCl}_3)$   $\delta$  –5.58, 16.93, 17.58, 18.20, 25.83, 46.94, 50.38, 64.04, 65.31, 66.77, 128.03, 128.30, 128.60, 135.57, 172.51, 174.19.

**g2(-COOH, -TBDMS), 6.**

**g2(-CO<sub>2</sub>C<sub>7</sub>H<sub>7</sub>, -TBDMS)** (30.0 g, 32.9 mmol) and Pd/C (1.5 g) were dissolved in EtOAc (100 ml) and hydrogenated according to the general procedure for the removal of the benzyl group. The yield was 26.2 g (97%) of a viscous and colorless liquid.  $^1\text{H-NMR}(\text{CDCl}_3)$   $\delta$  0.00 (s, 24H,  $-\text{Si}(\text{CH}_3)_2$ ), 0.84 (s, 36H,  $-\text{C}(\text{CH}_3)_3$ ), 1.06 (s, 6H,  $-\text{C}(\text{CH}_3)_2$ ), 1.25 (s, 3H,  $-\text{CH}_3$ ), 3.57–3.72 (q, 8H,  $-\text{CH}_2\text{O}-$ ), 4.06–4.29 (m, 4H,  $-\text{CH}_2\text{O}-$ ), 5.28 (s, 2H,  $-\text{CH}_2-$ ).  $^{13}\text{C-NMR}(\text{CDCl}_3)$   $\delta$  –5.59, 16.96, 17.55, 18.18, 25.81, 46.59, 50.41, 64.07, 64.92, 174.17, 178.84.

**g3(-CO<sub>2</sub>C<sub>7</sub>H<sub>7</sub>, -TBDMS), 7.**

$^1\text{H-NMR}(\text{CDCl}_3)$   $\delta$  0.00 (s, 48H,  $-\text{Si}(\text{CH}_3)_2$ ), 0.84 (s, 72H,  $-\text{C}(\text{CH}_3)_3$ ), 1.04 (s, 12H,  $-\text{CH}_3$ ), 1.09 (s, 6H,  $-\text{CH}_3$ ), 1.24 (s, 3H,  $-\text{CH}_3$ ), 3.59–3.72 (q, 16H,  $-\text{CH}_2\text{O}-$ ), 4.13–4.28 (q, 12H,  $-\text{C}(\text{CH}_3)_3$ ), 5.13 (s, 2H,  $-\text{CH}_2-$ ), 7.33 (s, 5H,  $-\text{Ph}$ ).  $^{13}\text{C-NMR}(\text{CDCl}_3)$   $\delta$  –5.58, 17.00, 17.48, 18.20, 25.84, 46.78, 50.32, 64.00, 64.81, 66.19, 67.14, 128.38, 128.45, 128.65, 135.42, 171.80, 174.03.

**g3(-COOH, -TBDMS), 8.**

$^1\text{H-NMR}(\text{CDCl}_3)$   $\delta$  0.00 (s, 48H,  $-\text{Si}(\text{CH}_3)_2$ ), 0.84 (s, 72H,  $-\text{C}(\text{CH}_3)_3$ ), 1.05 (s, 12H,  $-\text{CH}_3$ ), 1.20 (s, 6H,  $-\text{CH}_3$ ), 1.25 (s, 3H,  $-\text{CH}_3$ ), 3.58–3.73 (q, 16H,  $-\text{CH}_2\text{O}-$ ), 4.13–4.24 (q, 12H,  $-\text{CH}_2\text{O}-$ ).  $^{13}\text{C-NMR}(\text{CDCl}_3)$   $\delta$  –5.56, 17.00, 17.50, 18.23, 25.84, 46.27, 46.80, 50.37, 64.23, 64.97, 66.17, 67.90, 171.72, 173.30, 173.96.

### Dendrimer Like Star Synthesis

#### *A general procedure for polymerization of $\epsilon$ -caprolactone.*

The first generation dendrimer 6 0H (5.00 g, 7.64 mmol) was dried over MgSO<sub>4</sub> in warm THF, and filtered into the pre-flamed reaction flask, which was sealed after filling. The solvent was then evaporated under vacuum at 90 °C. Dry toluene (2 ml) was added and evaporated to remove residual H<sub>2</sub>O. This process was iterated three times. The reaction flask was filled with N<sub>2</sub>(g) and dry toluene (2 ml) to dissolve the initiator. The  $\epsilon$ -caprolactone (75.0 g, 658 mmol) was added and the temperature was increased to 110 °C and Sn(Oct)<sub>2</sub> (32 mg, 0.08 mmol) was added. The ratio of catalyst:initiator was 1:400. The polymerization was stirred for 24 h, diluted with THF and precipitated into cold MeOH to give 72.0 g (Yield: 90%) of a white crystalline powder.

<sup>1</sup>H-NMR (CDCl<sub>3</sub>) δ 1.30-1.42 (m, poly, -CH<sub>2</sub>-), 2.26-2.32 (t, poly, -CH<sub>2</sub>O-), 3.60-3.65 (t, 18H, -CH<sub>2</sub>OH-), 4.01-4.07 (t, poly, -CH<sub>2</sub>CO-), 4.33 (s, 12H, -CCH<sub>3</sub>(CH<sub>2</sub>O)<sub>2</sub>-), 6.88-7.24 (dd, 12H, Ph-). <sup>13</sup>C-NMR (CDCl<sub>3</sub>) δ 17.74, 24.50, 25.45, 28.27, 32.20, 34.03, 46.69, 51.58, 62.38, 64.05, 65.07, 120.67, 129.64, 146.22, 148.60, 171.37, 172.78, 173.65.

***A general procedure for the functionalization of poly(caprolactone) star polymer.***

Unfunctionalized **G-1 6 OH, 100** (8.00 g, 0.538 mmol), **g3(-TBDMS, -COOH)** (3.98 g, 4.84 mmol), triphenylphosphine (TPP) (1.69 g, 6.46 mmol) and diisopropyl azodicarboxylate (DIAD) (1.30 g, 6.46 mmol) were dissolved in THF (15 ml) according to the general procedure. After 12 h, the mixture was precipitated into cold MeOH. The yield was 10.56 g (99%) of a white crystalline powder. <sup>1</sup>H-NMR (CDCl<sub>3</sub>) δ 0.00 (s, 144H, -Si(CH<sub>3</sub>)<sub>2</sub>), 0.84 (s, 216H, -(CH<sub>3</sub>)<sub>3</sub>), 1.05 (s, 36H, -CH<sub>3</sub>), 1.20 (s, 18H, -CH<sub>3</sub>), 1.30-1.42 (m, poly, -CH<sub>2</sub>-), 1.57-1.69 (m, poly, -CH<sub>2</sub>), 2.26-2.32 (t, poly, -CH<sub>2</sub>O-), 3.57-3.72 (q, 48H, -CH<sub>2</sub>O-), 4.01-4.07 (t, poly, -CH<sub>2</sub>CO-), 4.10-4.26 (m, 24H, -CH<sub>2</sub>O-), 4.33 (s, 12H, -CH<sub>2</sub>O-), 6.91-7.09 (q, 12H, -Ph). <sup>13</sup>C-NMR (CDCl<sub>3</sub>) δ -5.59, 17.00, 17.59, 18.18, 24.55, 25.50, 25.81, 28.33, 34.09, 46.77, 50.38, 64.11, 64.89, 65.27, 120.72, 129.70, 146.26, 148.65, 171.40, 172.61, 172.83, 173.50, 174.15.

***A general procedure for the removal of the TBDMS group from the star polymer.***

Protected **G-1 6 OH, 100** (10.03 g, 0.52 mmol) was added to a sealed flask which was evacuated and filled with N<sub>2</sub>(g) (3x) to create an inert atmosphere. Dry CH<sub>2</sub>Cl<sub>2</sub> (30 ml) and BF<sub>3</sub>EtO<sub>2</sub> (0.37 g, 2.6 mmol) were then sequentially added. The mixture was stirred for 12 h at 40 °C before it was precipitated into cold MeOH. The filtered, dried product was 7.1 g (yield: 80%) of a white crystalline powder. <sup>1</sup>H-NMR (CDCl<sub>3</sub>) δ 1.04 (s, 36H, -CH<sub>3</sub>), (1.20 (s, 18H, -CH<sub>3</sub>, se NMR)) 1.32-1.42 (m, poly, -CH<sub>2</sub>), 1.57-1.69 (m, poly, -CH<sub>2</sub>CH<sub>2</sub>-), 2.26-2.32 (t, poly, -CH<sub>2</sub>O-), 3.63-3.84 (m, 48H, -CH<sub>2</sub>OH), 4.01-4.06 (t, poly, -CH<sub>2</sub>CO-), 4.13-4.24 (t, 48H, -CH<sub>2</sub>OCO-), 4.29-4.44 (m, 36H, -CH<sub>2</sub>O-), 6.91-7.09 (q, 12H, -Ph). <sup>13</sup>C-NMR (CDCl<sub>3</sub>) δ 17.03, 17.71, 18.00, 24.47, 25.43, 28.24, 34.01, 46.29, 46.68, 49.82, 64.04, 64.79, 65.13, 66.84, 120.66, 129.62, 146.21, 148.59, 171.36, 172.77, 172.94, 173.45, 174.89.

***G-1.5(0 OH) and a general procedure for AB<sub>2</sub> functionalization.***

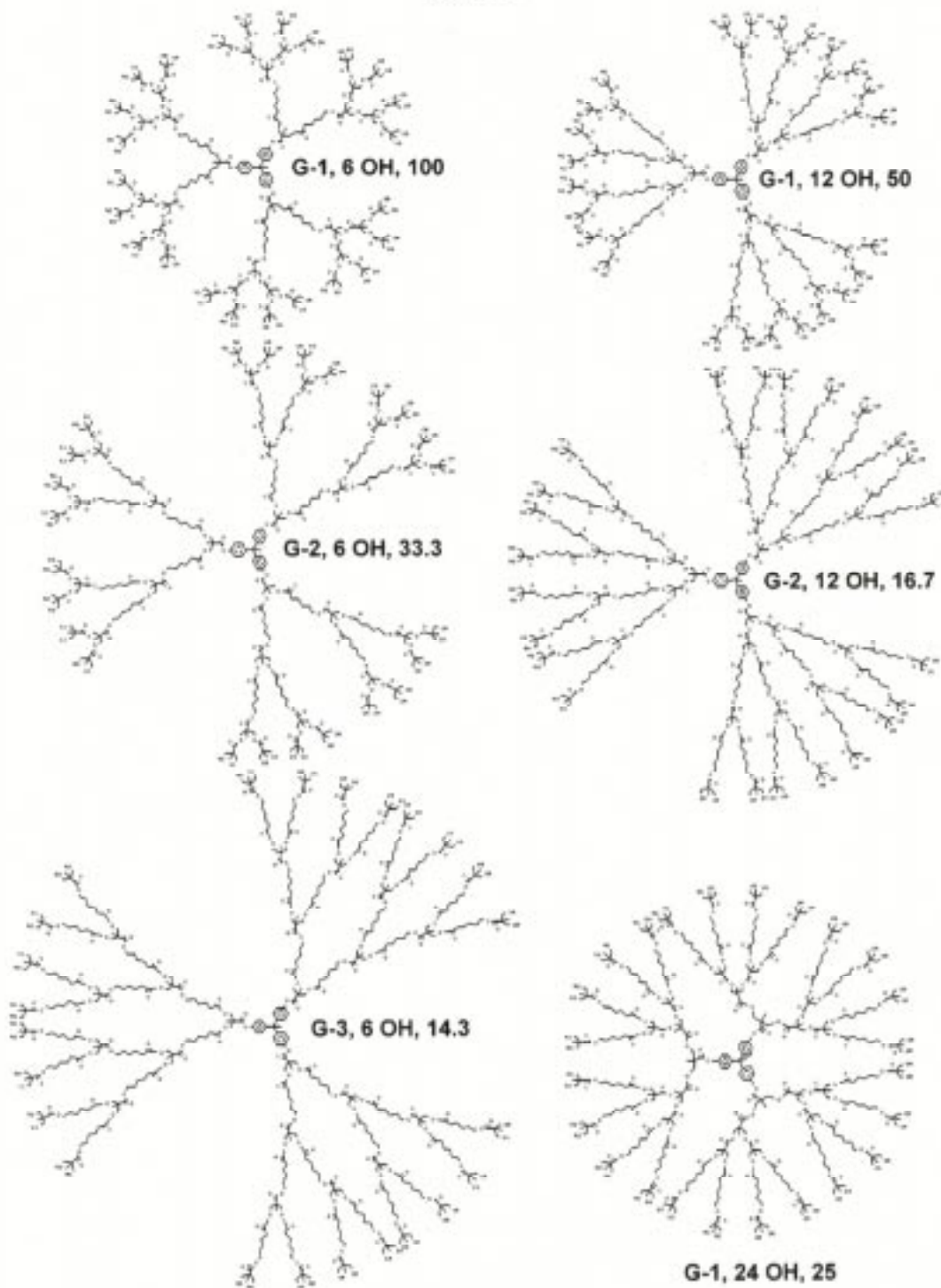
Diisopropyl azodicarboxylate (DIAD) (2.44 g, 12.1 mmol) at room temperature was slowly added to a stirred solution of **G-1(6 OH)**, M<sub>n</sub> = 14 300 g/mol (14.3 g, 1.00 mmol), **1** (2.01 g, 9.00 mmol), triphenylphosphine (TPP) (3.17 g, 12.1 mmol), and THF (5 mL). The reaction mixture was precipitated into cold methanol after 24 h. The filtered product was a white crystalline powder. Yield: 14.4 g (94%). Mp: 46.3 °C. <sup>1</sup>H-NMR (CDCl<sub>3</sub>) δ 0.96 (s, 18H, -CH<sub>3</sub>), 1.30 (m, poly, -CH<sub>2</sub>-), 1.60 (m, poly, -CH<sub>2</sub>CH<sub>2</sub>CH<sub>2</sub>-), 2.26 (t, poly, -COCH<sub>2</sub>-, J = 6.0 Hz), 3.55-4.60 (2d, 24H, -(CH<sub>2</sub>O)<sub>2</sub>CHPh, J = 9.2 Hz), 4.01 (t, poly, -CH<sub>2</sub>O-, J = 5.3 Hz), 4.14 (t, 12H, -CH<sub>2</sub>OCO), 4.31 (s, 12H, -CCH<sub>3</sub>(CH<sub>2</sub>O)<sub>2</sub>-), 5.37 (s, 6H, -CHPh), 6.88 (dd, 6H, Ph-, J = 6.8 Hz), 7.24 (dd, 6H, Ph-, J = 6.8 Hz), 7.25-7.36 (m, 30H, Ph-). <sup>13</sup>C-NMR (CDCl<sub>3</sub>) δ 17.87, 24.52, 25.48, 28.30, 34.06, 42.36, 46.73, 51.62, 64.06, 64.77, 65.14, 73.51, 101.69, 120.71, 126.17, 128.11, 128.87, 129.67, 137.92, 146.25, 148.64, 171.39, 172.78, 173.44, 173.95.

***G-1.5(12 OH) and a general procedure for removal of the benzylidene group.***

**G-1.5(0 OH)** (M<sub>n</sub> = 15 600 g/mol) (12.0 g, 0.77 mmol) was dissolved in THF (10 mL) and diluted with EtOAc (100 mL) before 1.0 g of Pd/C (10%) was added. The apparatus for catalytic hydrogenolysis was evacuated and filled with H<sub>2</sub>(g). The reaction mixture was stirred for 24 h, and the Pd/C was removed by filtration. The filtrate was precipitated into cold MeOH.

The filtered solid was a white crystalline powder. Yield: 10.0 g (86%). Mp: 49.7 °C.  $^1\text{H-NMR}$  ( $\text{CDCl}_3$ )  $\delta$  0.99 (s, 18H,  $-\text{CH}_3$ ), 1.29 (m, poly,  $-\text{CH}_2-$ ), 1.56 (m, poly,  $-\text{CH}_2\text{CH}_2\text{CH}_2-$ ), 2.21 (t, poly,  $-\text{COCH}_2-$ ,  $J = 5.9$  Hz), 3.00 (t, 12 OH,  $-\text{OH}$ ), 3.61–3.81 (2d, 24H,  $-\text{CH}_2\text{OH}$ ,  $J = 5.2$  Hz), 4.01 (t, poly,  $-\text{CH}_2\text{O}-$ ,  $J = 5.2$  Hz), 4.06 (t, 12H,  $-\text{CH}_2\text{OCO}$ ), 4.26 (s, 12H,  $-\text{CCH}_3(\text{CH}_2\text{O})_2-$ ), 6.84 (dd, 6H, Ph–,  $J = 6.9$  Hz), (dd, 6H, Ph–,  $J = 6.9$  Hz).  $^{13}\text{C-NMR}$  ( $\text{CDCl}_3$ )  $\delta$  17.13, 17.74, 24.50, 25.46, 28.14, 34.04, 46.69, 49.20, 51.60, 64.06, 64.56, 65.12, 67.68, 120.68, 129.65, 146.23, 148.61, 171.37, 172.78, 173.45 175.77.

Scheme 1

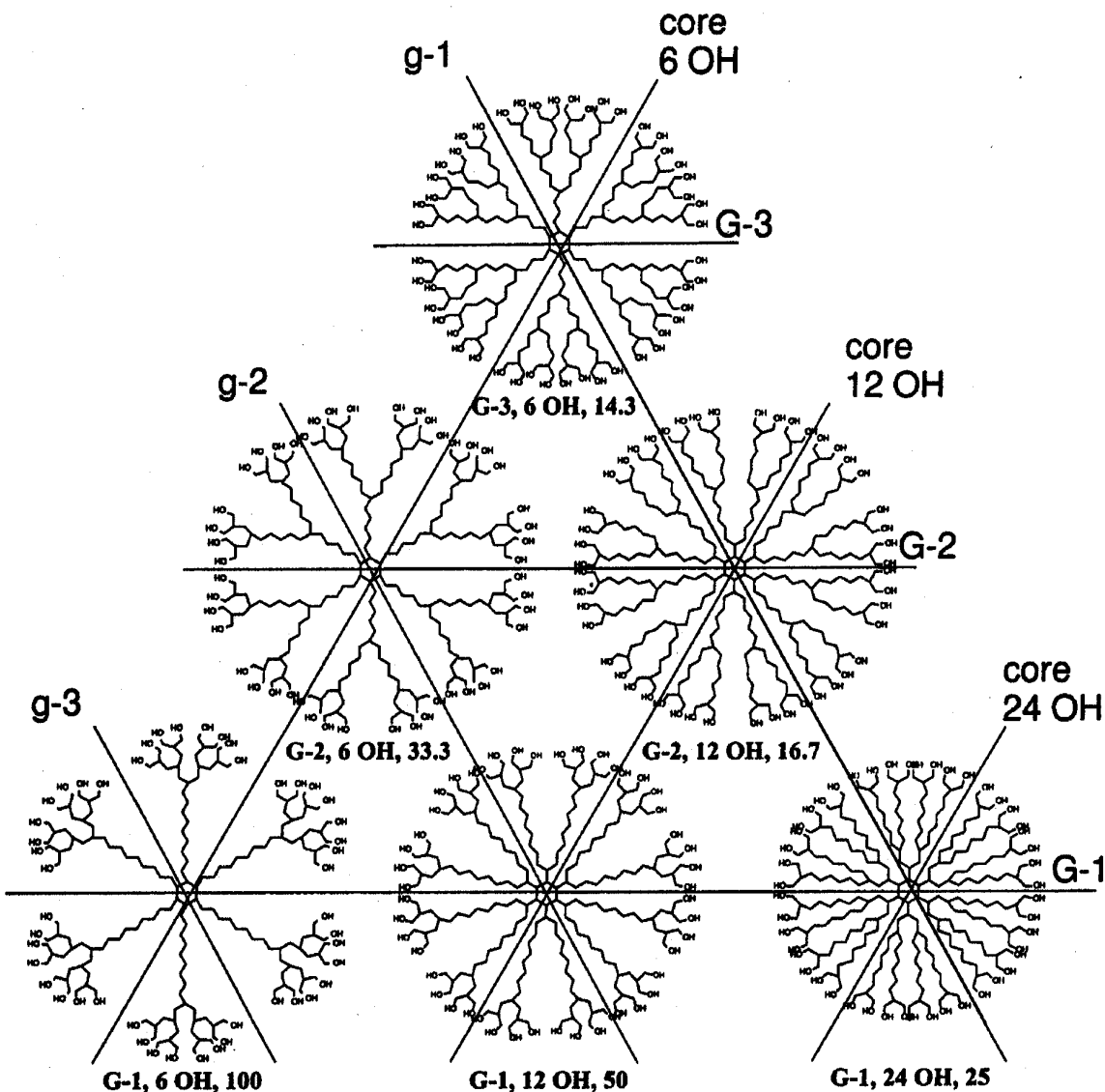


## RESULTS AND DISCUSSION

Six constitutional isomers of dendrimer-like star polymers were designed and synthesized (Scheme 1). The polymers were constructed from generations of high molecular weight polymer with branching junctures derived from bis(hydroxymethyl) propionic acid (bis-MPA), emanating radially from a dendritic central core.

Poly( $\epsilon$ -caprolactone) was used as the polymeric building block, a concept that has been reported earlier for the generation of star, hyperbranched and dendrimer-like star polymers.<sup>11</sup> The living ring-opening polymerization (ROP) initiated from the bis(hydroxymethyl) groups produces polymer with accurate control of molecular weight, molecular weight distribution, and end-group functionality. The constitutional isomers were designed to have number average molecular weights of 79,500 g/mol with 45 branching junctures and 48 hydroxyl end-groups. At a first glance at Scheme 1, the polymers appear to be randomly designed with branching concentrated

**Scheme 2**



either at the surface, the central region or throughout the polymer. A closer look at the triangular arrangement of the polymers in Scheme 2 reveals the strategy in the design. From the top to the bottom left corner of the triangle, each of the polymers have six arm star poly( $\epsilon$ -caprolactone) in the central core initiated from the first generation dendrimer, denoted as line 6-OH. Likewise, the line denoted as 12-OH represents the polymers initiated from the second generation dendrimer, whereas line 24-OH denotes the polymer initiated from the third generation dendrimer. Moving down the triangle from the top to the bottom right corner, these polymers each have the first generation dendron at the polymer surface (line g-1). Likewise, the lines denoted as g-2 and g-3 are polymers that have the second or third generation dendrons at the surface, respectively. The horizontal lines denoted as G-1 through G-3 indicate the number of generations of poly( $\epsilon$ -caprolactone) or the degree of internal branching (Scheme 2).

The target design and structure of the six isomers are detailed in Table 1. The polymers are organized by generation of poly( $\epsilon$ -caprolactone) denoted as either G-1, G-2 or G-3 which have been initiated from either the first, second or third generation bis-MPA dendrimer, denoted 6-OH, 12-OH and 24-OH respectively (Scheme 3), and the average degree of polymerization for the poly( $\epsilon$ -caprolactone). The terminology referring to the polymers will reflect this organization: for example, polymer **G-1, 6-OH, 100** indicates a single generation of polycaprolactone, G-1, initiated from the first generation dendrimer, 6-OH, and the 100 represents the average target degree of polymerization (DP) per arm. The six arms give a total average degree of polymerization for the isomers of 600. To obtain the same overall molecular weight for all of the isomers, the average targeted degree of polymerization per arm was adjusted accordingly to account for the functionality of the initiator and the number of generations of the isomer (Table 1). For instance, initiation from the first, second or third generation dendrimer required targeted average DPs of 100, 50 and 25, respectively. For the isomers with more than one generation of poly( $\epsilon$ -caprolactone), the average degree of polymerization was held constant throughout the generations (Table 1). Also shown in Table 1 are the surface dendrons used for each polymer, denoted as g-1 through g-3 (Scheme 4), required to bring the total surface functionality to 48.

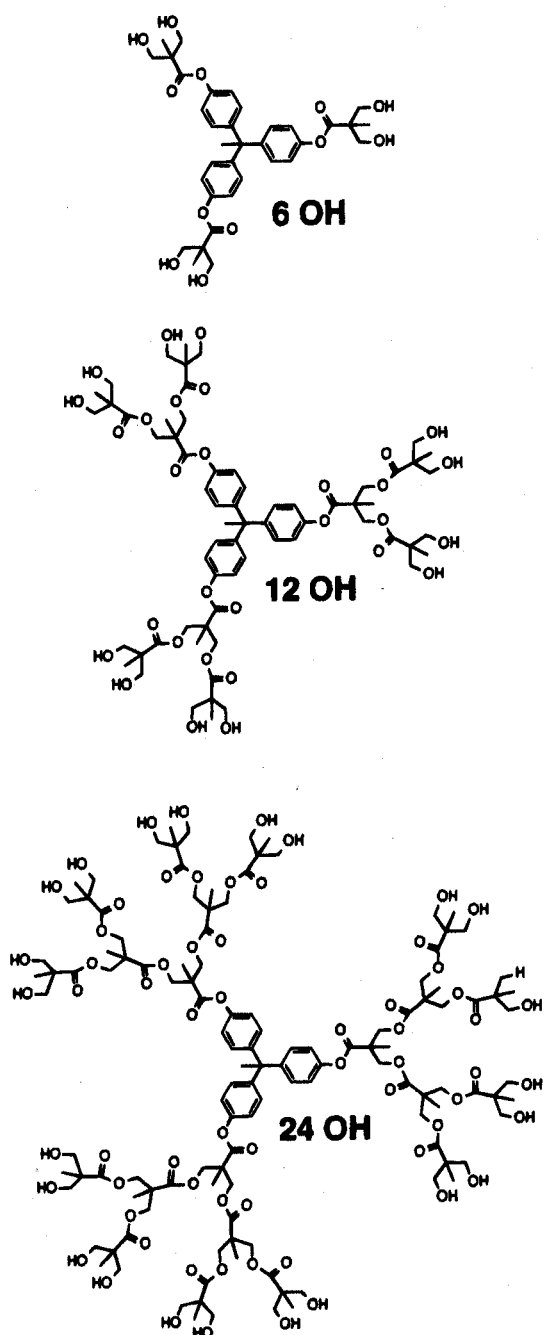
**Table 1. Design and Structure of the Six Isomeric Polymers**

Polymer	G1, 6OH, 100	G1, 12OH, 50	G1, 24OH, 25	G2, 6OH, 33.3	G2, 12OH, 16.7	G3, 6OH, 14.3
DP/arm	100	50	25	33.3	16.7	14.3
Core	6 OH	12 OH	24 OH	6 OH	12 OH	6 OH
Surface Dendron	g-3	g-2	g-1	g-2	g-1	g-1
Number of arms (G1/G2/G3)	6	12	24	6/12	12/24	6/12/24
M <sub>n</sub> , target R= SiR <sub>3</sub>	79 400	79 400	79 400	79 400	79 400	79 400
M <sub>n</sub> , target R= OH	73 900	73 900	73 900	73 900	73 900	73 900

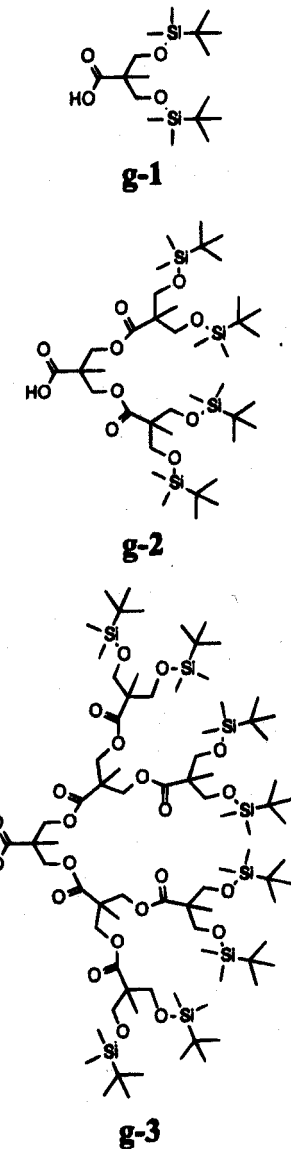
The first, second and third generation dendrimers of bis-MPA (Scheme 3) were synthesized by procedures developed by Hult et al.<sup>13</sup> Fortunately,  $\epsilon$ -caprolactone dissolves the dendritic initiators allowing bulk polymerizations. In some cases, approximately 5% toluene was

added to mediate the viscosity, and the concentration of  $\text{Sn}(\text{Oct})_2$  relative to the initiating alcohol was kept as low as possible.<sup>6f</sup> For each dendrimer surveyed, the initiation of  $\epsilon$ -caprolactone proved to be facile and gave the desired star-shaped polymers, with accurate control of molecular weight and extremely narrow polydispersities.

**Scheme 3**



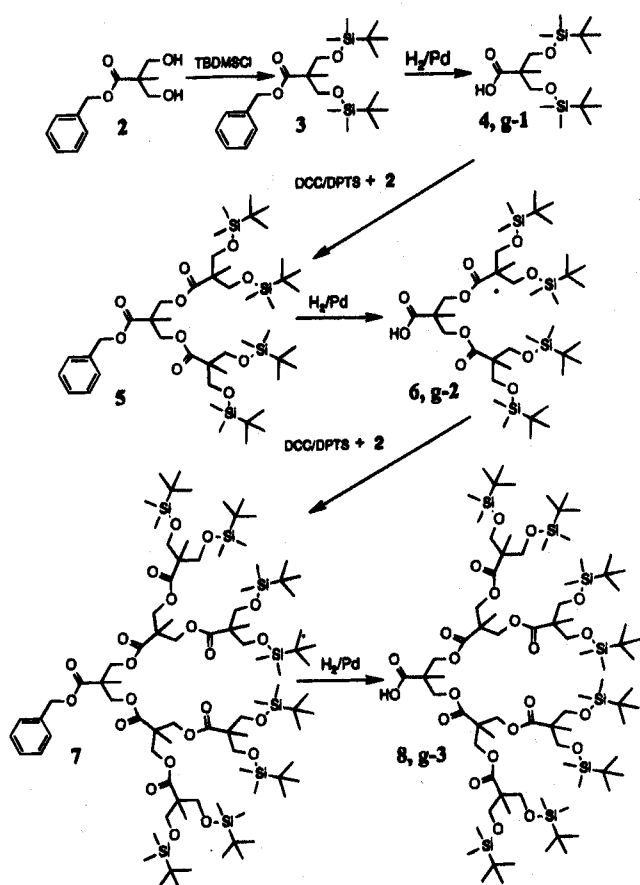
**Scheme 4**



In addition to the use of dendrimers, functional dendrons were also prepared and used as “building blocks” to obtain molecular architectures that more closely resemble that of the most advanced dendrimers (Scheme 4). The benzylidene-protected bis-MPA, **1**, was synthesized in

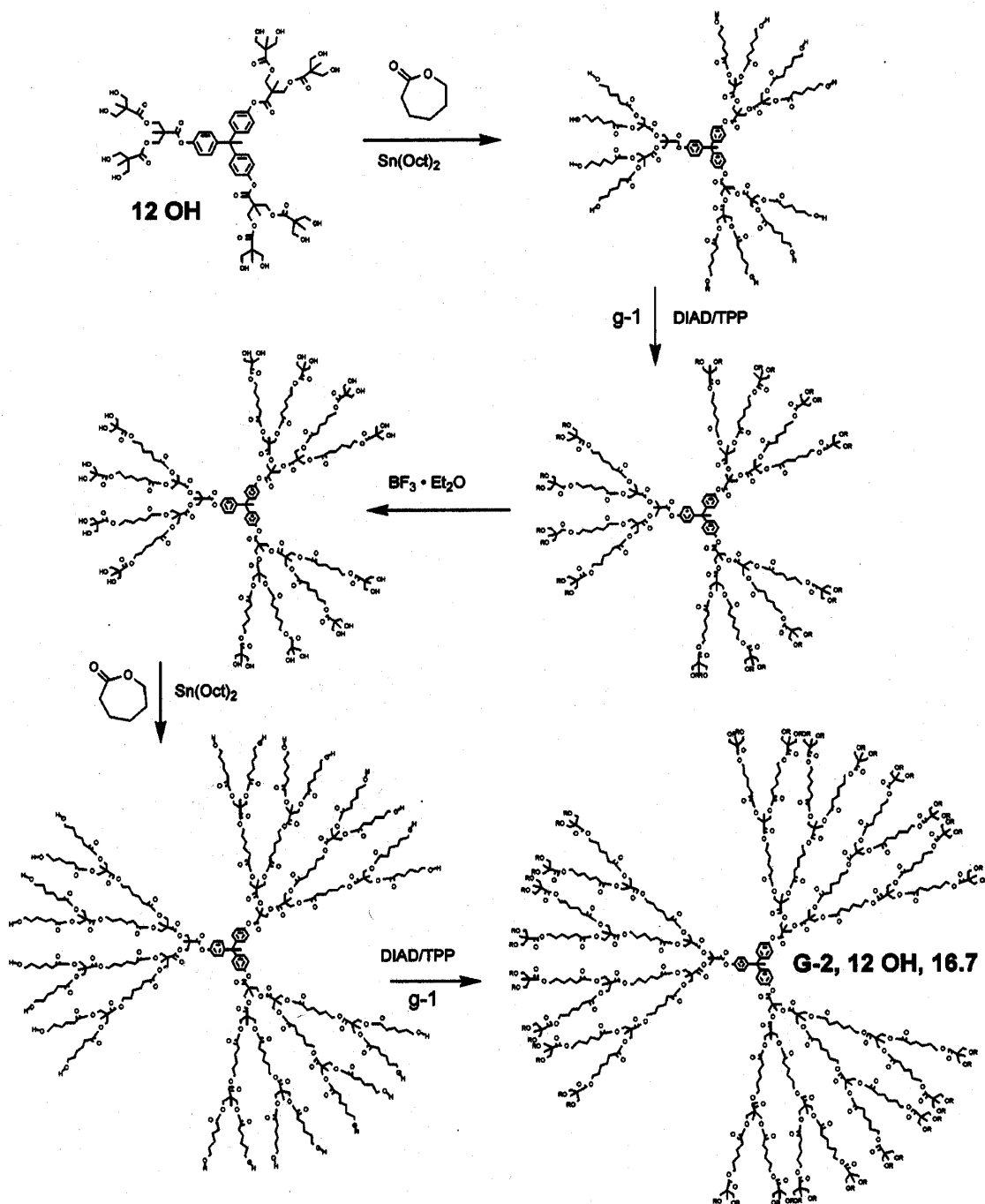
one step from the reaction bis-MPA and benzaldehyde dimethyl acetal according to a literature procedure.<sup>11a</sup> The tert-butyldimethylsilyl protected bis-MPA and the second and third generation acid functional dendrons derived from it were obtained from the divergent growth approach and also used to modify the surface functionality of the star polymers. The dendrons were synthesized by the convergent growth approach (Scheme 5).<sup>11b</sup> The hydroxyl groups of the benzyl ester **2** were protected with *tert*-butyldimethylsilyl chloride (TBDMSCl) to give **3**. The benzyl group could then be selectively removed by catalytic hydrogenation to give the free acid **4**, which was then coupled with **2** to afford the second-generation dendron **5**. This in turn could be readily hydrogenolyzed to give **6 (g-2)**. The third-generation dendron was synthesized by the coupling of **2** with **6**. Deprotection by hydrogenolysis gave the requisite dendron **8 (g-3)**. The structure of the dendrons were confirmed by <sup>1</sup>H-NMR and <sup>13</sup>C-NMR.

**Scheme 5**



A typical synthesis for a dendrimer-like star polymer having two generations of poly( $\epsilon$ -caprolactone) is provided. Dendrimer **12-OH** was used as the “initiator” to generate a 12 arm star poly( $\epsilon$ -caprolactone). The hydroxyl functional polymer was prepared in bulk at 100 °C using stannous-2-ethylhexanoate ( $S_n(Oct)_2$ ) as the catalyst. The number average molecular weight was 24,100 g/mol as determined by <sup>1</sup>H-NMR and the molecular weight distribution as measured by size exclusion chromatography (SEC) was 1.06. The hydroxy functional arms had an average degree of polymerization (DP) of 17.1 (target DP = 16.7). The polymer was further

Scheme 6

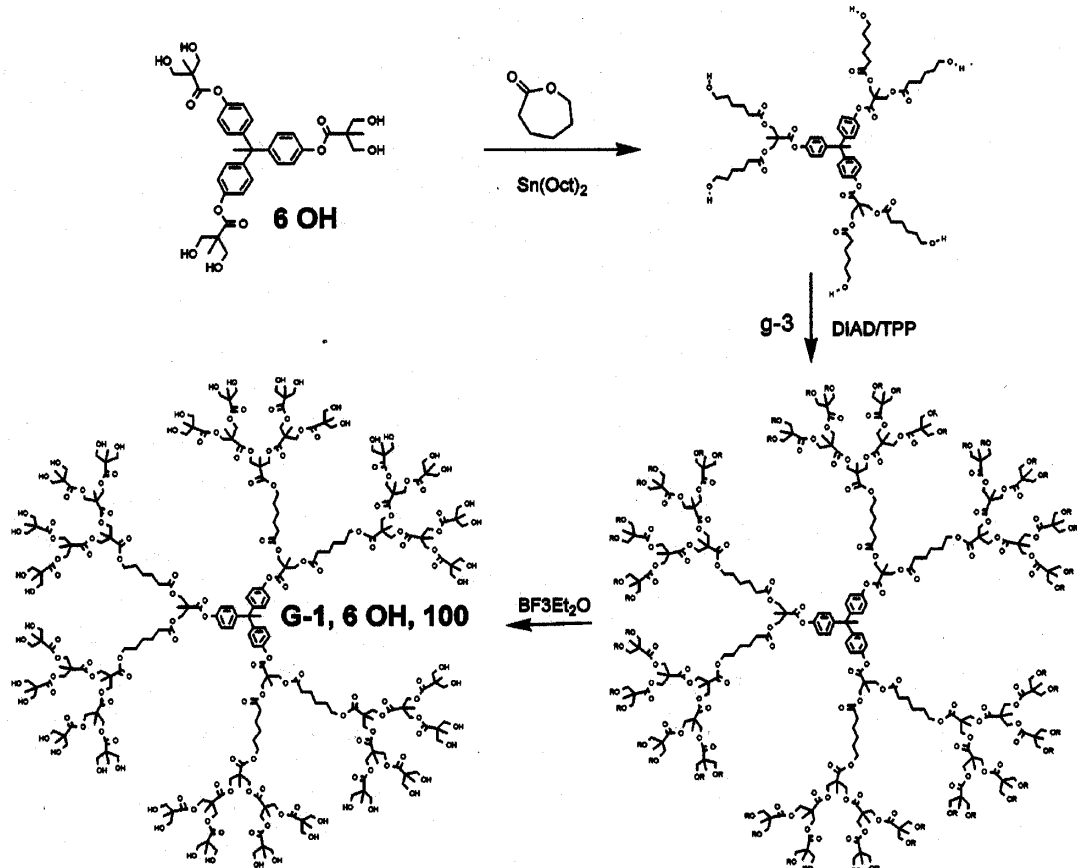


functionalized with **1** using diisopropyl azodicarboxylate (DIAD) and triphenylphosphine (TPP) in dry THF.<sup>11a</sup> The benzylidene protecting groups were removed by hydrogenolysis to generate a 6 arm star polymer containing 24 hydroxyl groups. This polymer was used as a “macroinitiator” for the ring-opening polymerization of  $\epsilon$ -caprolactone to give the second generation dendrimer-like star polymer. The DP of the second generation (DP)<sub>2</sub> and, if required, the third generation (DP)<sub>3</sub> were calculated from the following equation:<sup>11a</sup>

$$x = a(DP)_1 + b(DP)_2 + c(DP)_3 \quad (2)$$

where  $x$  is the summed integrated area of any specific repeating unit of the monomer for all generations in the specific polymer, and **a**, **b**, and **c** are the integrated areas of the chain ends of the first, second, and third generations, respectively. To calculate the DP of the second and third generation, it was assumed that the DP's of the inner generations were unchanged and that all chain ends had initiated polymerization. These assumptions lead to the relation,  $\mathbf{a} = \mathbf{b}/2 = \mathbf{c}/4$ . In addition, it was assumed that the protons of the chain ends and the protons of the repeating units have equivalent relaxation times ( $\tau$ ). The average DP of the 24 arms in the second layer was determined to be 16.0 by  $^1\text{H-NMR}$ : a value which corresponds well with the target value of

**Scheme 7**



16.7. This gave a total molecular weight for polymer of 71,400 g/mol, and the molecular weight distribution as measured by SEC was 1.12. Each arm was again functionalized with **1** and deprotected to bring the total surface hydroxyl functionality to 48, and the molecular weight to 80,100 g/mol. It should be pointed out that the only purification required after polymerization, functionalization, and deprotection was a simple precipitation into cold methanol.

The most difficult transformation in the preparation of the dendrimer-like star isomers was the functionalization of the arms with the high average DP's to obtain the requisite branching and functionality content (such as **G-1, 6-OH, 100**). For example, the preparation of **G-1, 6-OH, 100** from the third generation dendron (g-3) was particularly difficult due to the high molecular weight of the poly( $\epsilon$ -caprolactone) (Scheme 7). In this particular case, DCC and DPTS conditions were used to couple the acid-functional dendrons with the hydroxyl-functional poly( $\epsilon$ -caprolactone) to produce the forty-eight hydroxyl-functional dendrimer-like star

polymer.<sup>11b</sup> The extent of coupling was followed by <sup>1</sup>H-NMR and <sup>13</sup>C-NMR spectroscopy. The <sup>13</sup>C-NMR spectra for **G-1**, **6-OH**, **100**, a mixture of **G-1**, **6-OH**, **100** and **g-3** and the transformation are shown in Figure 1. Quantitative functionalization is confirmed by the complete shift of the CH<sub>2</sub>OH signal from 62 ppm upon esterification of the hydroxyl groups. Shown in Figure 2 are the <sup>1</sup>H-NMR spectra of three tert-butyldimethylsilyl protected dendrimer-like star polymers. The spectra are shown to display some of the differences between the selected isomers. In all spectra, the resonances associated with the major peaks of poly( $\epsilon$ -caprolactone) (1.35, 1.60, 2.25, 4.05 ppm) and the protecting group (0.00, 0.90 ppm) are clearly observed. In addition, the methylene protons from the protected bis-MPA on the surface have the same chemical shift (3.62 ppm). The variation in the chemical structure of the isomers can

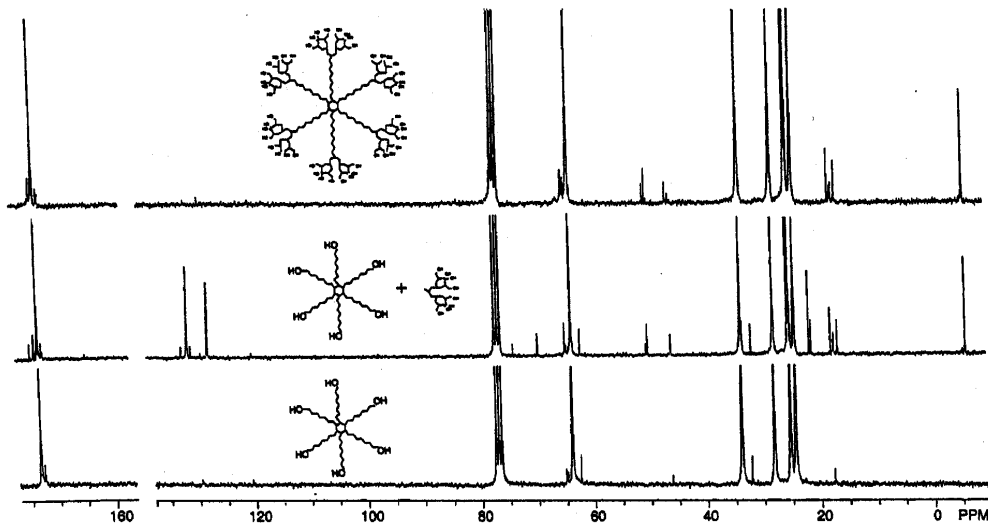


Figure 1. <sup>13</sup>C NMR spectra of (bottom) unfunctionalized **G-1**, **6 OH** **100**, (middle) a mixture of unfunctionalized **G-1**, **6 OH** **100** with **g-3** and (top) **G-1**, **6 OH**, **100**.

be detected from the chemical shifts of the bis-MPA methylene protons inside the isomers (4.00–4.35 ppm) as well as from the methyl protons of bis-MPA at 1.00–1.25 ppm. The resonances of the –CH<sub>3</sub> protons reveal each generation of bis-MPA in the three isomers, as previously reported.<sup>11a,b</sup> The –CH<sub>3</sub> protons connected to the core are hidden under the poly( $\epsilon$ -caprolactone) peak at 1.35 ppm.

The tert-butyldimethylsilyl protecting groups were removed with BF<sub>3</sub> · EtO<sub>2</sub> to give the requisite forty-eight hydroxyl groups along the periphery of the dendrimer-like star polymers. Shown in Figure 3 are the <sup>1</sup>H-NMR spectra of selected dendrimer-like star polymers after deprotection, and the disappearance of the peaks at 0 and 0.84 ppm is consistent with deprotection. Likewise, the <sup>13</sup>C-NMR spectra showed no signs of the protecting group and the quaternary carbon of the bis-MPA in the outer layer of the dendron was shifted quantitatively.

The theoretical and experimental number average molecular weights as measured by <sup>1</sup>H-NMR spectroscopy and SEC for both the protected and deprotected isomers are shown in Table 1. The number average molecular weights by <sup>1</sup>H-NMR are in good agreement with the target values, consistent with the high level of control in these polymerizations and transformations. The molecular weights from SEC, relative to poly(styrene) standards, are also in the appropriate range. Clearly, SEC is a measure of the hydrodynamic volume and the comparison of linear standards with these complex architectures is difficult. Nonetheless, the polymers show extremely narrow polydispersities (Table 2) and monomodal distributions. The combined data

from SEC and  $^{13}\text{C}$ -NMR and  $^1\text{H}$ -NMR spectroscopy clearly indicate that all the constitutional isomers have the requisite complex structure.

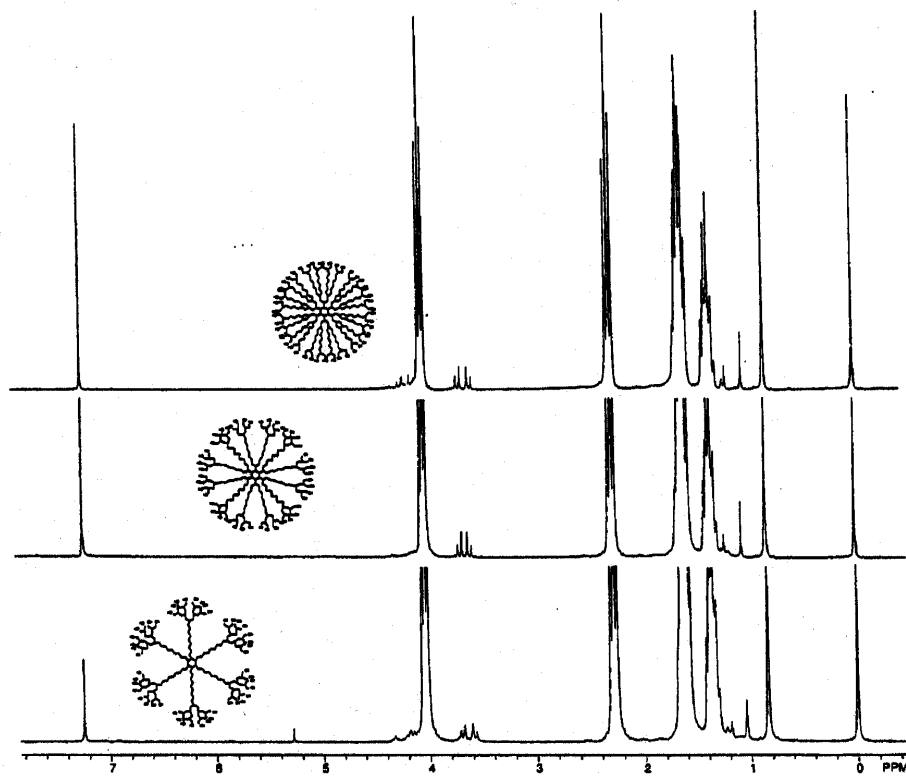


**Figure 2.**  $^1\text{H}$  NMR spectra of selected dendrimer-like star polymers; (bottom) G-1, 24 OH, 100, (middle) G-1, 12 OH, 50, and (top) G-1, 24 OH, 25.

A closer look at the SEC data of the different isomers reveals some interesting trends. Although each of the polymers have nearly identical molecular weights calculated from  $^1\text{H}$ -NMR measurements, their molecular weights, or more appropriately, hydrodynamic volumes, measured by SEC vary somewhat (Table 2). Examination of the isomers initiated from the first generation dendrimer show differences only in the generation of poly( $\epsilon$ -caprolactone) employed. For example, Figure 4 shows the SEC chromatograms of one of the triangle (Scheme 2), denoted as line 6 OH in which the branching density and generation of caprolactone are varied. Despite having nearly identical number average weights, their hydrodynamic volumes vary when compared in this way (Scheme 2). In this case, moving down the triangle, larger hydrodynamic volumes are realized. Clearly, the polymers with multiple generations of poly( $\epsilon$ -caprolactone) have a more compact structure, and the plot of the number average molecular weight, measured by SEC, versus the generation of poly( $\epsilon$ -caprolactone) in the dendrimer-like star polymers demonstrates this point (Figure 5). However, for a given generation of poly( $\epsilon$ -caprolactone), the placement of the branching (i.e., at the core or the periphery of the macromolecule) has a minimal effect on the hydrodynamic volume. For example, shown in Figure 6 (also Table 1) are the SEC chromatograms for the first generation dendrimer-like star isomers, **G-1, 6 OH, 100**, **G-1, 12 OH, 50** and **G-1, 24 OH, 25** (the samples along the line denoted as G-1 in Scheme 2) in which minimal differences in hydrodynamic volumes can be observed.

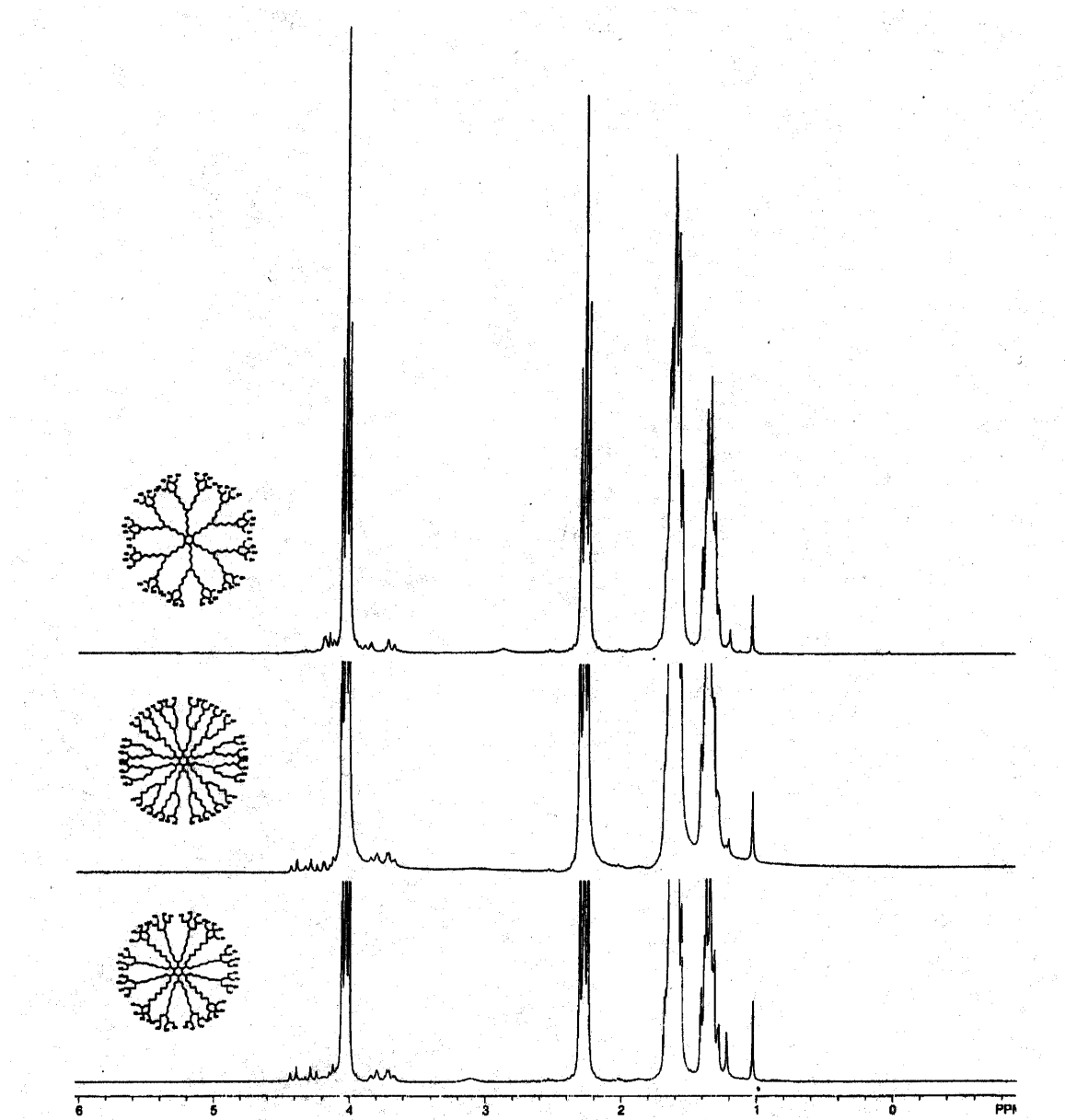
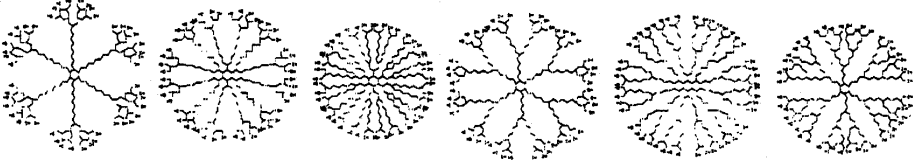


Figure 3:  $^1\text{H}$  NMR spectra of selected deprotected dendrimer-like star polymers; (bottom G-1, 12 OH, 50, (middle) G-2, 12 OH, 16.7 and (top) G-2, 6 OH, 33.

More rigorous measurement of the hydrodynamic radius  $R_h$  from DLS is given in Table 3 along with the radius of gyration  $R_g$  from SAXS data. The self-consistent field model of de Gennes and Hervet predicts a dense core for such a structure, relating the hydrodynamic radius of the macromolecule to the molar mass as  $R_g \sim M^{0.2}$ ,<sup>15a</sup> whilst the computational study of starburst molecules by Lescanec and Muthukumar favours an aggregation of molecular material at the shell, leading to a relation with a higher scaling exponent:  $R_g \sim M^{0.5}$ .<sup>15b</sup> As a further contrast, the molecular dynamics simulation of Murat and Grest predicts a relatively space filled structure (irrespective of solvent conditions) where  $R_g \sim M_n^{0.33}$ .<sup>12b</sup> The results of this work, where the scaling exponents vary between 0.34 and 0.363 (Table 3), agree well with this latter study, and therefore suggest a compact, space filled architecture of the dendrimer-like star polymers, exhibiting a relatively uniform density profile from the core to the periphery. A similar finding

has been made by Scherrenberg *et al* in modelling the radial density profile of poly(propyleneimine) dendrimers up to the fifth generation; the density profile matched the compact conditions rather than either the shell weighted or core weighted models.<sup>12g</sup>

Table 2. Characteristics of the Six Isomeric Polymers



Polymer	G1, 6OH, 100	G1, 12OH, 50	G1, 24OH, 25	G2, 6OH, 33.3	G2, 12OH, 16.7	G3, 6OH, 14.3
$M_n$ , <sup>1</sup> H-NMR R= SiR <sub>3</sub>	79 600	79 500	79 800	79 700	80 100	80 200
$M_n$ , SEC R= SiR <sub>3</sub>	96 700	93 400	97 400	91 500	83 600	78 200
$M_n$ , <sup>1</sup> H-NMR R= OH	74 100	74 100	74 300	74 200	74 600	74 700
$M_n$ , SEC R= OH	85 900	84 700	87 700	84 700	76 300	72 400
$M_w/M_n$	1.09	1.04	1.08	1.15	1.12	1.19
$T_m$ (°C) R= SiR <sub>3</sub>	56	53	52	52	51	42
$T_m$ (°C) R= OH	57	55.5	54	51	50	43
$T_g$ (°C), R= OH	-55	-54	-55	-54	-53	-55

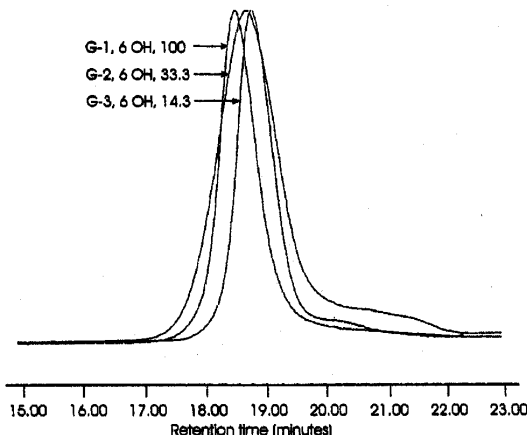


Figure 4. SEC chromatograms of the dendrimer-like star polymers organized in Scheme 2 along the line denoted as **6**.

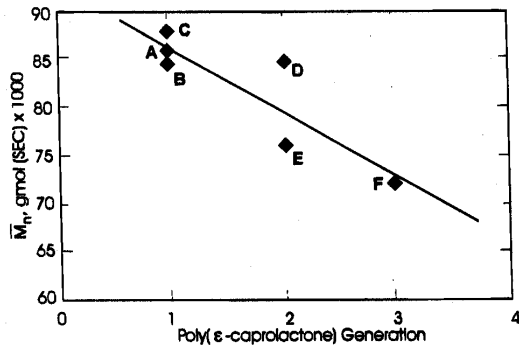


Figure 5. Number-average molecular weight  $M_n$  versus the different generations of poly(ε-caprolactone) in the dendrimer-like star polymers; (A) G-1, 6 OH 100, (B) G-1 12 OH, 50, (C) G-1, 24 OH, 25, (D) G-2, 6 OH, 33.3, (E) G-2 12 OH 16.7, (F) G-3, 6 OH 14.3.

It is possible to investigate differences in radial density distribution within the different isomeric architectures. We consider this architecture in the light of the radial density distribution of polymer segments within a multiple arm star  $\rho(r)$  over radial distance  $r$ , as described by Daoud and Cotton:<sup>15c</sup>

$$\rho(r) = \int f^{(3v-1)/2} r^{(1-3v)/v} dr \quad (3)$$

where  $f$  denotes the number of arms of the star polymer and  $v$  denotes the Flory exponent. In our case, we employ the knowledge that THF acts as a good solvent for this system: thus  $v = 3/5$ . The number of arms in the star is not constant by reason of the dendritic junctions, but is rather a function of the radius. Thus, for our purposes we are enabled to consider the profile in discrete

stages between the 6 arm core and 48 end groups at the surface and note the number of arms  $f(r)$  existent at that stage. This yields a single value density index:

$$\rho(r) = \sum f(r)^{2/3} r^{-4/3} \quad (4)$$

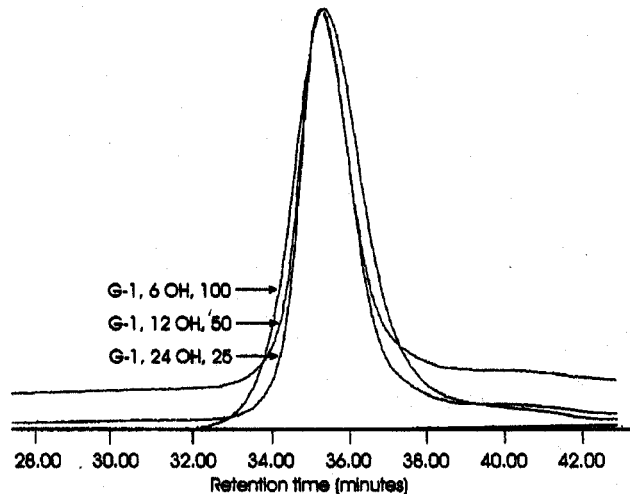


**Figure 6.** SEC chromatograms of the dendrimer-like star polymers organized in Scheme 2 along the line denoted as G-1.

A shortcoming of these calculations is that it ignores spatial mixing between generations, i.e. it assumes that each new generation begins at the same radius from the core. This source of uncertainty will affect the lowest density polymers most but will be minimized in the case of the good solvent, which we consider in this work. The resulting density indices are listed in Table 3. The results show that the **G-1, 6 OH, 100** isomer has the lowest density, whilst the **G-1, 24 OH, 25** isomer has the highest density. These predictions correlate intuitively with the architectures of the isomers as shown in Scheme 2: we can ascribe the low density of **G-1, 6 OH, 100** to its unique six long, (DP 100) caprolactone arms, and the high density of **G-1, 24 OH, 25** to its unique high functionality ( $f = 24$ ) core.

**Table 3. Conformational and Structural Properties of Dendrimer-like Star Isomers**

polymer	$M_n$ ( $^1\text{H}$ NMR)	$R_g$ Å (SAXS)	$R_h$ Å (DLS)	$R_h/R_g$	$X$ ( $R_g = \frac{M_n}{M_n^*}$ )	density index, $\rho$
<b>G-1, 6 OH, 100</b>	79 600	54.4	72	1.32	0.354	6.58
<b>G-1, 12 OH, 50</b>	79 600	52.0	69	1.33	0.350	8.53
<b>G-1, 24 OH, 25</b>	79 800	46.1	86	1.87	0.339	11.6
<b>G-2, 6 OH, 33.3</b>	79 700	60.0	84	1.40	0.363	6.67
<b>G-2, 12 OH, 16.7</b>	80 100	50.0	75	1.50	0.346	8.55
<b>G-3, 6 OH, 14.3</b>	80 200	50.0	71	1.42	0.346	7.30

We also utilize these density values as a means to observe variations from the star polymer model within the different architectures of the polycaprolactone isomers. Figure 7 shows the scaling exponents of the isomer series in the relation between radius of gyration (from SAXS data) and number average molecular weight (from  $^1\text{H}$ -NMR data) as a function of the density index. All six exponents are close to the value of  $1/3$  theoretically predicted for a compact structure.<sup>12b</sup> Furthermore it is possible to observe a trend within the experimental values shown in Figure 7 with a positive slope in the relationship between  $x$  and  $1/\rho$ . This confirms the

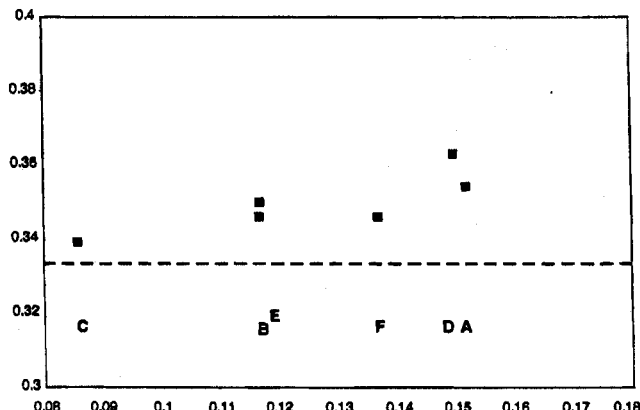


**Figure 7.** Scaling exponent  $x$  of the relationship  $R_g \sim M_n^x$  against  $1/\rho$ , where  $\rho$  is a theoretical density index calculated from the radial density distribution of a star polymer (see text). (A) G-1, 6 OH 100, (B) G-1 12 OH, 50, (C) G-1, 24 OH, 25, (D) G-2, 6 OH, 33.3, (E) G-2 12 OH 16.7, (F) G-3, 6 OH 14.3. The broken line indicates the anticipated value from a compact, space filled star polymer.

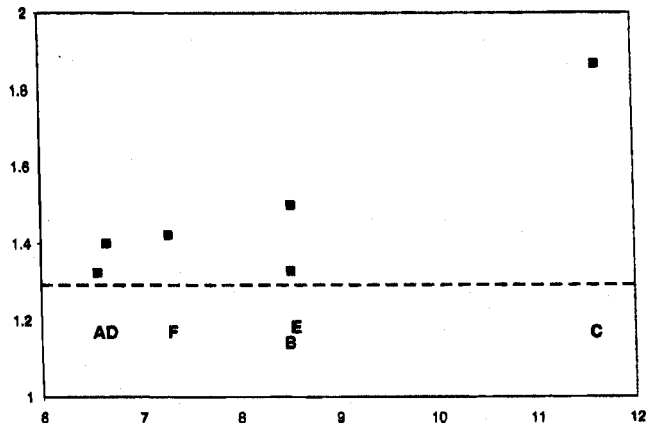
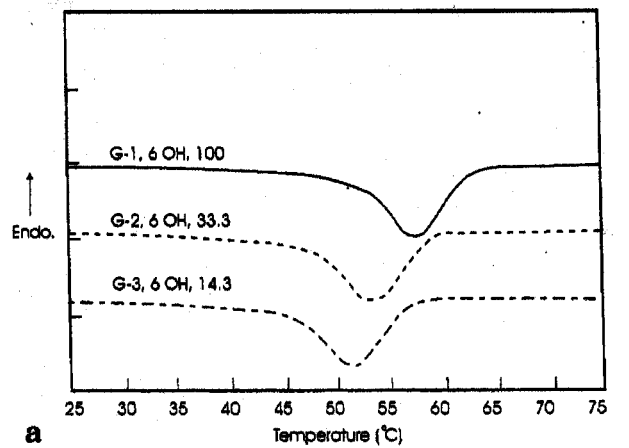


**Figure 8.** Ratio of the hydrodynamic radius from DLS to the radius of gyration from SAXS ( $R_h/R_g$ ), against a theoretical density index  $\rho$  calculated from the radial density distribution of a star polymer: (A) G-1, 6 OH 100; (B) G-1 12 OH, 50; (C) G-1, 24 OH, 25; (D) G-2, 6 OH, 33.3; (E) G-2 12 OH 16.7; (F) G-3, 6 OH 14.3. The broken line indicates the anticipated value for a star polymer:  $R_h = R_g \sqrt{(5/3)}$ .

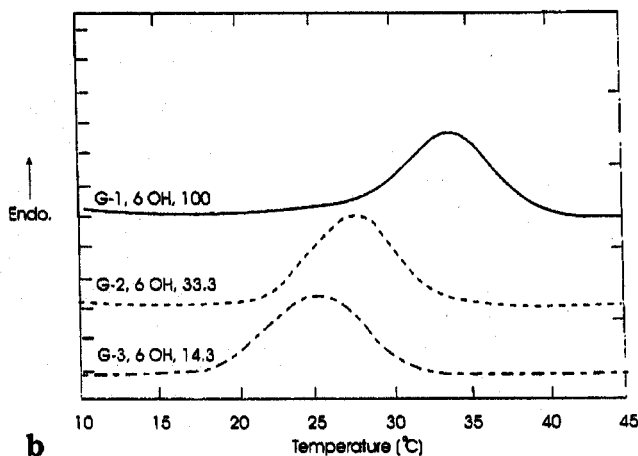
theoretical prediction: that the density is most core weighted for **G-1, 24 OH, 25**, with the radial density distribution becoming more shell weighted, (i.e. the exponent increases towards  $1/2$ ), with decreasing density index. These results are also intuitively reasonable: **G-1, 24 OH, 25** has the most compact structure from its high functionality core whilst **G-1, 6 OH, 100** and **G-2, 6 OH, 33.3** are seen to be the most shell weighted from Scheme 2, and predicted to be the least dense according to Equation 4. Accordingly, these two isomers, **G-1, 6 OH, 100** and **G-2, 6 OH, 33.3**, possess the largest scaling exponents of radius of gyration to molecular weight.

We also consider the ratio of the hydrodynamic radius to the radius of gyration as a measure of the radial density distribution of the isomers. In the case of the compact structure, which the results considered above suggest these isomers possess (Table 3, Figure 7), the relation between  $R_h$  and  $R_g$  should follow the form:  $R_h \approx \sqrt{(5/3)} R_g$ , where the coefficient, initially  $\sqrt{(5/3)}$  should increase with core density. Figure 8 shows the ratio  $R_h/R_g$  as a function of the theoretical density index  $\rho$ , with  $R_h$  measurements extracted from DLS data and  $R_g$  measurements extracted from SAXS data. The results of Figure 8 harmonize well with those of Figure 7: all the isomers show good approximations to the compact structure (star) model, (the ratio of  $\sqrt{(5/3)}$  is shown with the broken line). Once again, as with Figure 7, the trend between the isomers relating  $R_g$  to the molecular weight with the most differing architectures is evident from Figure 8: **G-1, 6 OH, 100** and **G-2, 6 OH, 33.3** possess the most shell weighted density distributions, as indicated by the lower values of the  $R_h/R_g$  ratio (Figure 8), and **G-1, 24 OH, 25**, possesses the most core weighted density distribution. These experimental data also show good agreement with the star model of radial density distribution.

All of the dendrimer-like star isomers were semi-crystalline, as measured by differential scanning calorimetry (DSC) measurements. Shown in Table 2 is a summary of these data for the isomers with and without the tert-butyldimethylsilyl protecting groups. Each of the isomers have  $T_g$  between  $-57$  and  $-59^\circ\text{C}$  analogous to their linear analog  $-57^\circ\text{C}$ , and  $T_g$  did not vary with the functionality of the end groups. The melting points and enthalpy varied significantly from each other and linear poly( $\epsilon$ -caprolactone)  $T_m = 60^\circ\text{C}$ , consistent with different degrees of crystallization. As a general trend, the melting point decreases as one proceeds up the triangle of structures along the horizontal lines denoted as G-1, G-2 and G-3 (Scheme 2). This trend is

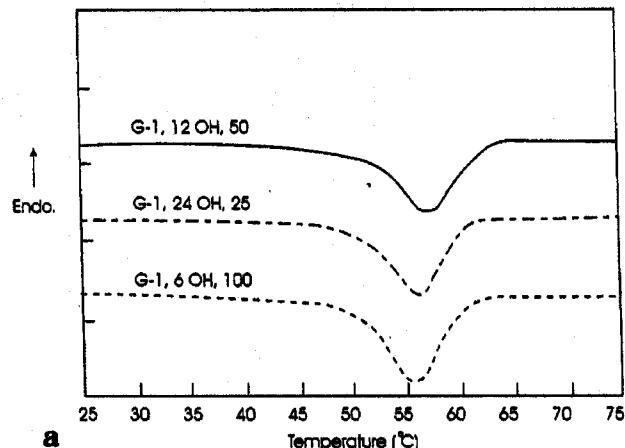


a

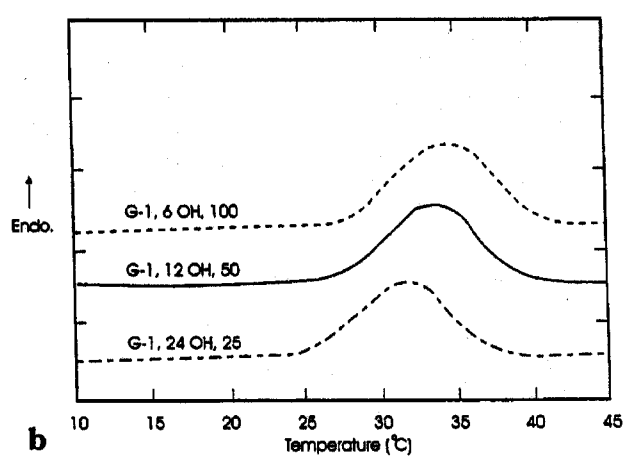


b

**Figure 9.** (a) DSC thermograms of dendrimer-like star polymers organized in Scheme 2 along the line denoted as 6 OH (a) melting region and (b) crystallization region. (b) DSC thermograms of dendrimer-like star polymers organized in Scheme 2 along the line denoted as 6 OH (a) melting region and (b) crystallization region.



a



b

**Figure 10.** (a) DSC thermograms of dendrimer-like star polymers organized in Scheme 2 along the line denoted as G-1 (a) melting region and (b) crystallization region. (b) DSC thermograms of dendrimer-like star polymers organized in Scheme 2 along the line denoted as G-1 (a) melting region and (b) crystallization region.

clearly observed in the calorimetry plots for the melting and crystallization thermograms of the polymers **G-1, 6 OH, 100**, **G-2, 6 OH, 33.3** and **G-3, 6 OH, 14.3** along line **6 OH** from Scheme 2 (Figures 9a and 9b). However, within a given generation of poly( $\epsilon$ -caprolactone), the differences in the thermal behavior was minimal. Shown in Figures 10a and 10b are the calorimetry data for the samples along line **G-1** from Scheme 2, in which minimal differences in the crystallization and melting temperatures are observed. These data are corroborated by the enthalpy measurements for both the crystallization and melting transitions. Shown in Figure 11 are the enthalpy measurements of the dendrimer-like star isomers for both the protected and unprotected end groups. The enthalpy values for the isomers vary significantly from the top to the bottom of either side of the triangle. Higher generations of poly( $\epsilon$ -caprolactone), exhibited lower enthalpies of crystallization or melting, yet within a given generation of poly( $\epsilon$ -caprolactone) the differences were minimal. Similar trends were observed for both types of end-group functionalities, and the differences in the crystallization and melting enthalpies between the two end groups was minimal. Therefore, the morphology appears to be strongly dependent on the generation of poly( $\epsilon$ -caprolactone) and placement of branching points rather than on the degree of

polymerization. The conclusions are supported by crystallization studies of hyperbranched poly( $\epsilon$ -caprolactone) prepared from AB<sub>2</sub> macromonomers. Here the morphology was found to strongly depend on the average DP between branching junctions and, above a critical DP, the crystallization temperatures and enthalpies were identical. These data are consistent with the observations of Hawker et al.<sup>9</sup> in the comparison of an amorphous dendrimer  $T_g = 42^\circ\text{C}$  with the exact linear analog which is highly crystalline. Here branching played a significant role in the mechanical properties as well as the hydrodynamic volume. Other differences between the

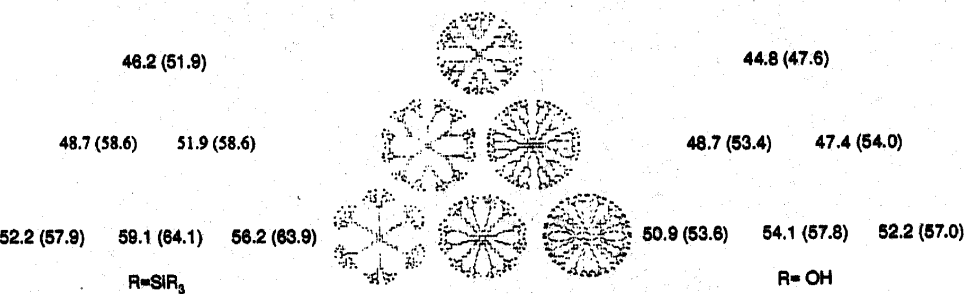


**Figure 11.** Melting enthalpies for both the protected and deprotected dendrimer-like star polymers organized according to Scheme 2. Crystallization enthalpies are given in parentheses.

constitutional isomers including the end groups were subtle. The differences in melting points, crystallization temperatures and  $T_g$  of the six isomers with free or protected end groups was minimal: presumably a consequence of the high molecular weight isomers (Table 2). All the isomers formed tough, opaque, ductile films, as expected with a semi-crystalline morphology.

## SUMMARY

The design and synthesis of six isomers of dendrimer-like star polymers is described. The polymers were constructed from poly( $\epsilon$ -caprolactone) with branching junctures derived from bis-MPA. Various generations of dendrimers, dendrons and poly( $\epsilon$ -caprolactone) strategically placed together produced the six constitutional isomers with forty-five branching junctions, forty-eight surface hydroxyl groups and number average molecular weights in the proximity of 80,000 with narrow polydispersities (1.08–1.19). The melting point and degree of crystallinity appeared to strongly depend on the generations of poly( $\epsilon$ -caprolactone). The branched architectures produced melting points and temperatures that were all broad and diffuse, consistent with a perturbed morphology.

DLS measurements yielded values of the hydrodynamic radius  $R_h$  which, when combined with values of the radius of gyration  $R_g$  from SAXS measurements, showed that the radial density distribution of molecular material was consistent with a many arm star polymer, and was not significantly biased towards core-dense or shell dense distributions. A form of the Daoud-Cotton model for the radial density distribution of star polymers gave good agreement with experimentally determined values. Trends within the radial density distributions were consistent with the designed architectures.

## ACKNOWLEDGMENT

The authors gratefully acknowledge partial support for this work from the NSF Center for Polymer Interfaces and Macromolecular Assemblies (CPIMA) under cooperative agreement DMR-9400354. MT thanks The Swedish Foundation for International Cooperation in Research and Higher Education (STINT) for fellowship support. JAP acknowledges the support of the Stanford Synchrotron Radiation Laboratory in providing facilities used in these experiments: this work was supported by Department of Energy contract DE-AC03-76SF00515.

## REFERENCES

1. (a) Webster, O. W. *Science* **1994**, *251*, 887. (b) Fréchet, J. M. J. *Science* **1994**, *263*, 1710. (c) Hedrick, J. L.; Miller, R. D.; Hawker, C. J.; Carter, K. R.; Volksen, W.; Yoon, D. Y.; Trollsås, M. *Adv. Mater.* **1998**, *10*, 1049.
2. Nasipuri, D. In *Stereochemistry of Organic Compounds*; John Wiley & Sons: New Delhi, 1991.
3. (a) Patten, T. E.; Matyjaszewski, K. *Adv. Mater.* **1998**, *10*, 901. (b) Matyjaszewski, K. *Controlled Radical Polymerization*; Matyjaszewski, K., Ed.; ACS Symposium Series No. 685, American Chemical Society, Washington, D.C. 1998. (c) Percec, V.; Barboiu, B.; Kim, H.-J. *J. Am. Chem. Soc.* **1998**, *120*, 305. (d) Kato, M.; Kamigaito, M.; Sawamoto, M.; Higashimura, T. *Macromolecules* **1995**, *28*, 1721. (e) Moineau, G.; Granel, C.; Dubois, P.; Jérôme, R.; Teyssié, P. *Macromolecules* **1998**, *31*, 542. (f) Granel, C.; Dubois, P.; Jérôme, R.; Teyssié, P. *Macromolecules* **1996**, *29*, 8576. (g) Uegaki, H.; Kotani, Y.; Kamigaito, M.; Sawamoto, M. *Macromolecules* **1997**, *30*, 2249. (h) Matyjaszewski, K. *Macromolecules* **1998**, *31*, 4710. (i) Ando, T.; Kato, M.; Kamigaito, M.; Sawamoto, M. *Macromolecules* **1996**, *117*, 5614. (j) Hawker, C. J. *J. Am. Chem. Soc.* **1994**, *116*, 11314. (k) Georges, M. K.; Veregin, R. P. N.; Kazmaier, P. M.; Hamer, G. K. *Macromolecules* **1993**, *26*, 2987. (l) Keoshkerian, B.; Georges, M. K.; Boils-Boissier, D. *Macromolecules* **1995**, *28*, 6381. (m) Hawker, C. J. *Acc. Chem. Res.* **1997**, *30*, 373. (n) Hawker, C. J.; Fréchet, J. M. J.; Grubbs, R. B. *J. Am. Chem. Soc.* **1995**, *117*, 10763. (o) Benoit, D.; Grimaldi, S.; Finet, J. P.; Tordo, P.; Fontanille, M.; Gnanou, Y. *Polym. Prep.* **1997**, *38*, 729. (p) Puts, R. D.; Sogah, D. Y. *Macromolecules* **1996**, *29*, 3323. (q) Kazmaier, P. M.; Daimon, K.; Georges, M. K.; Hamer, G. K.; Veregin, R. P. N. *Macromolecules* **1997**, *30*, 2228.
4. (a) Fréchet, J. M. J.; Hawker, C. J. In *Comprehensive Polymer Science 2nd Supp.*; Aggarwal, S. L., Rosso, S., Eds.; Pergamon Press: London, 1996; p. 71. (b) Tomalia, D. A.; Dupont Durst, H. Topics in *Current Chemistry* **1993**, *165*, 193. (c) Frey, H.; Lach, C.; Lorentz, K. *Adv. Mater.* **1998**, *10*, 279. (d) Gorman, C. *Adv. Mater.* **1998**, *10*, 295. (e) Fischer, M.; Vogtle, F. *Angew. Chem. Int. Ed. Engl.* **1999**, *38*, 885. (f) Webster, O. W. *Science* **1994**, *251*, 887. (g) Fréchet, J. M. J. *Science* **1994**, *263*, 1710. (h) Frey, H. *Angew. Chem. Int. Ed. Engl.* **1998**, *37*, 2193.
5. Devonport, W.; Hawker, C. J. *Polymer News* **1996**, *21*, 370.
6. (a) Rempp, P.; Franta, E. *Adv. Polym. Sci.* **1984**, *58*, 1. (b) Simms, J. A.; Spinelli, H. J. *J. Coat. Technol.* **1987**, *59*, 126. (c) Johansson, M.; Trollsås, M.; Hult, A. *J. Polym. Sci.: Part A: Polym. Chem.* **1992**, *30*, 2203. (d) Roovers, J.; Zhou, L. L.; Toporowski, P. M.; Van der Zwan, M.; Iatrou, H.; Hadjichristidis, N. *Macromolecules* **1993**, *26*, 4324. (e) Vasilenko, N. G.; Rebrov, E. A.; Muzafarov, A. M.; Ebwein, B.; Striegel, B.; Möller, M. *Macromol. Chem. Phys.*

1995, 199, 881. (f) Trollsås, M.; Hedrick, J. L.; Mecerreyes, D.; Dubois, P.; Jerome, R.; Ihre, H.; Hult, A. *Macromolecules* 1997, 30, 8508. (g) Ueda, J.; Kamigaito, M.; Sawamoto, M. *Macromolecules* 1998, 31, 6762. (h) Angot, S.; Murthy, K. S.; Taton, D. Gnaou, Y. *Macromolecules* 1998, 31, 7218. (i) Kim, S. H.; Han, Y. K.; Ahn, K.-D.; Kim, Y. H.; Chang, T. *Makromol. Chem.* 1993, 194, 3229. (j) Tian, D.; Dubois, P.; Jérôme, R.; Tessié, P. *Macromolecules* 1994, 27, 4134. (k) Lambert, O.; Dumas, P.; Hurtrez, G.; Riess, G. *Macromol. Rapid Commun.* 1997, 18, 343. (l) Trollsås, M.; Atthoff, B.; Claesson, H.; Hedrick, J. L. *Macromolecules* 1998, 31, 4390. (m) Trollsås, M.; Hedrick, J. L. *Macromolecules* 1998, 31, 3439. (n) Trollsås, M.; Hawker, C. J.; Remenar, J. F.; Hedrick, J. L.; Johansson, M.; Ihre, H.; Hult, A. *J. Polym. Sci., Chem. Ed.* 1998, 36, 2793. (o) Vasilenko, N. G.; Rebrov, E. A.; Muzafarov, A. M.; Esswein, B.; Striegel, B.; Möller, M. *Macromol. Chem. Phys.* 1998, 199, 889. (p) Heise, A.; Hedrick, J. L. Trollsås, M.; Miller, R. D.; Frank, C. W. *Macromolecules* 1999, 32, 231. (q) Heise, A.; Hedrick, J. L.; Miller, R. D.; Frank, C. W. *J. Am. Chem. Soc.* (in press).

7. (a) Vert, M.; Li, S. M.; Spenlehauer, G.; Guerin, P. *J. Mater. Sci., Mater. Med.* 1992, 3, 432. (b) Peppas, A.; Langer, R. *Science* 1994, 263, 1715. (c) Langer, R. *Nature Supp.* 1998, 5, 392.

8. Johnson, L. K.; Killian, C. M.; Brookhart, M. *J. Am. Chem. Soc.* 1995, 117, 6414.

9. (a) Hawker, C. J.; Malmström, E. E.; Frank, C. W.; Kampf, J. P. *J. Am. Chem. Soc.* 1997, 119, 9903. (b) Mio, C.; Kiritsov, S.; Thio, Y.; Brafman, R.; Prausnitz, J.; Hawker, C. J.; Malmström, E. *J. Chem. Eng. Data* 1998, 43, 541.

10. (a) Moreno-Bondi, M. D.; Orellana, G.; Turro, N. J.; Tomalia, D. A. *Macromolecules* 1990, 23, 912. (b) Naylor, A. M.; Goddard, W. A. III; Kiefer, G. E.; Tomalia, D. A. *J. Am. Chem. Soc.* 1989, 111, 2339. (c) Hawker, C. J.; Farrington, P.; Mackay, M.; Fréchet, J. M. J.; Wooley, K. L. *J. Am. Chem. Soc.* 1995, 117, 6123. (d) Devadoss, C.; Bharathi, P.; Moore, J. S. *Angew. Chem. Int. Ed. Engl.* 1997, 36, 1633. (e) Wooley, K. L.; Hawker, C. J.; Pochan, J. M.; Fréchet, J. M. J. *Macromolecules* 1993, 26, 1514. (f) Fields, H. R.; Kowalewski, T.; Schaefer, J.; Wooley, K. L. *ACS Polym. Prep.* 1998, 39(2), 1169.

11. (a) Trollsås, M.; Hedrick, J. L. *J. Am. Chem. Soc.* 1998, 120, 4644. (b) Trollsås, M.; Claesson, H.; Atthoff, B.; Hedrick, J. L. *Polym. Prepr. Angew. Chem. Int. Ed. Engl.* 1998, 37, 3132. (c) Trollsås, M.; Claesson, H.; Atthoff, B.; Hedrick, J. L.; Pople, J. A.; Gast, A. P. (submitted 1999). (d) Hedrick, J. L.; Trollsås, M.; Hawker, C. J.; Atthoff, B.; Claesson, H.; Heise, A.; Miller, R. D.; Mecerreyes, D.; Jérôme, R.; Dubois, P. *Macromolecules* 1998, 31, 8691. (e) Trollsås, M.; Kelly, M. A.; Claesson, H.; Siemens, R.; Hedrick, J. L. *Macromolecules* 1999, published on the Web. (f) Trollsås, M.; Atthoff, B.; Hedrick, J. L. 1999 (in preparation).

12. (a) Mansfield, M. L.; Klushin, L. I. *Macromolecules* 1993, 26, 4262. (b) Murat, M.; Grest, G. S. *Macromolecules* 1996, 29, 1278. (c) Lue, L.; Prausnitz, J. M. *Macromolecules* 1997, 30, 6650. (d) Chen, Z. Y.; Cui, S.-M. *Macromolecules* 1996, 29, 7943. (e) Prosa, T. J.; Bauer, B. J.; Amis, E. J.; Tomalia, D. A.; Scherrenberg, R. *J. Polym. Sci. B* 1997, 35, 2913. (f) Ramzi, A.; Scherrenberg, R.; Brackman, J.; Joosten, J.; Mortensen, K. *Macromolecules* 1998, 31, 1621. (g) Scherrenberg, R.; Coussens, B.; van Vliet, P.; Edouard, G.; Brackman, J.; de Brabander, E.; Mortensen, K. *Macromolecules* 1998, 31, 456.

13. (a) Ihre, H.; Hult, A. *Polym. Mat. Sci. Eng.* 1997, 77, 71. (b) Ihre, H.; Hult, A.; Soderlind, E. *J. Am. Chem. Soc.* 1996, 118, 6388.

14. (a) Provencher, S. W.; Hendrix, J.; DeMaeyer, L.; Paulussen, N. *J. Chem. Phys.* **1978**, *69*, 4273. (b) Provencher, S. W.; *Comput. Phys. Commun.* **1982**, *27*, 213. (c) Provencher, S. W. *Comput. Phys. Commun.* **1982**, *27*, 229.

15. (a) de Gennes, P. G.; Hervet, H.; *J Phys. Lett. (Paris)* **1983**, *44*, 351. (b) Lescanec, R. L.; Muthakumar, M.; *Macromolecules* **1990**, *23*, 2280. (c) Daoud, M.; Cotton, J. P.; *J Phys. (Paris)* **1982**, *43*, 531.